JGR Earth Surface

RESEARCH ARTICLE
10.1029/2018JF004990

Sedimentological and Geochemical Composition of Aeolian Sediments in the Taklamakan Desert: Implications for Provenance and Sediment Supply Mechanisms

Qida Jiang[1,3,4] and **Xiaoping Yang**[2]

[1]Key Laboratory of Cenozoic Geology and Environment, Institute of Geology and Geophysics, Chinese Academy of Sciences, Beijing, China, [2]Department of Geography, School of Earth Sciences, Zhejiang University, Hangzhou, China, [3]University of Chinese Academy of Sciences, Beijing, China, [4]Institutions of Earth Sciences, Chinese Academy of Sciences, Beijing, China

Key Points:
- Sedimentological, geochemical, and geomorphological methods are combined to decipher sediment provenance and supply mechanisms
- For Taklamakan, main sources of the sand fraction and the dust fraction are the Kunlun, and the Kunlun and Tian Shan Mountains, respectively
- Inferences of sediment provenance and supply mechanisms may be strongly dependent on the grain size of the sediment being analyzed

Supporting Information:
- Supporting Information S1
- Table S1
- Table S2
- Table S3

Correspondence to:
X. Yang,
xpyang@zju.edu.cn

Citation:
Jiang, Q., & Yang, X. (2019). Sedimentological and geochemical composition of aeolian sediments in the Taklamakan Desert: Implications for provenance and sediment supply mechanisms. *Journal of Geophysical Research: Earth Surface*, *124*, 1217–1237. https://doi.org/10.1029/2018JF004990

Received 28 DEC 2018
Accepted 9 APR 2019
Accepted article online 16 APR 2019
Published online 22 MAY 2019

Abstract Sediment provenance is a key issue in understanding the aeolian system of the Taklamakan Desert, an important source of global dust and the largest sand sea in the midlatitudes worldwide. In provenance research, it may be a mistake to assume that the sand and dust fractions of desert sediments have the same source, which has been the case in previous studies of the Taklamakan Desert. The aims of the present study were to identify the provenance of the sand and dust fractions of the sediments of the Taklamakan Desert, to determine the contemporary sediment supply mechanisms of the desert, and to assess the relative importance of silt-producing mechanisms for the desert dust. We analyzed the grain size of desert sediment samples and measured the content of major, trace, and rare earth elements within the bulk samples, sand fractions (>63 μm), and dust fractions (<63 μm). Our grain size and geochemical data sets suggest that the Kunlun Mountains are the main source of the sand fraction, whereas both the Kunlun and Tian Shan Mountains are the main sources of the dust fraction. Our interpretation is supported by the elevation gradient within the Taklamakan Desert and by wind data.

1. Introduction

Determining sediment provenance is indispensable for assessing the state of an aeolian system (Kocurek & Lancaster, 1999; Muhs et al., 2017), and it provides basic information for studies of the sedimentology, geomorphology, and climatology of deserts. Knowledge of the environmental evolution of arid and semiarid areas is important for sustainable development, and it has been a major research topic during the past few decades (Lancaster, 1995; Lancaster et al., 2016; Thomas, 2013; Wang et al., 2012; Yang & Eitel, 2016). The precise significance of sedimentary records for environmental evolution cannot be fully determined without knowledge of sediment provenance (Muhs et al., 2017; Thomas, 2013). Furthermore, the identification of different source-sink linkages for sandy sediments could lead to very different interpretations of regional sedimentary sequences (Hu & Yang, 2016). For example, the sand in desert marginal sequences may indicate a humid environment with direct sediment input from sandy alluvium and colluvium eroded from the uplands (Williams, 2015), whereas sands in the interior of deserts may indicate an arid environment with aeolian sediment input from desert dunes (Yang, Preusser, et al., 2006). Relatively little research has been done on modern sediment provenance in dryland areas, compared with Quaternary aeolian sequences (Thomas, 2013). Lancaster (2013) emphasizes that the provenance of desert sediments is a key issue in current aeolian research. And Muhs (2017) pointed out that more research should be undertaken on the topic, despite many challenges of determining sediment provenance in a dune field.

Desert sediments are mainly composed of sand and dust (silt and clay) particles, with the sand/silt boundary being widely defined at 63 μm (Bullard & Livingstone, 2009; Goudie & Middleton, 2006). The sand and dust fractions of aeolian desert sediments exhibit fundamentally different behavior: sand is transported predominantly by saltation over short distances (a few centimeters to meters in once hop) and close to the surface (~3 m), whereas dust moves mainly in suspension and can be transported over considerable distances (kilometers to thousands of kilometers) and across a large altitudinal range (Bullard & Livingstone, 2009; Nickling & Neuman, 2009; Pye, 1987). In provenance research, the sand fraction, which comprises a large

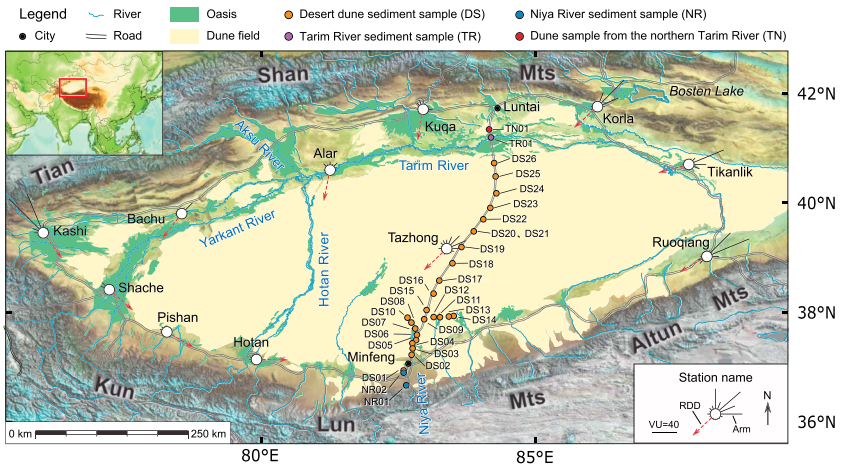

Figure 1. Map of the Tarim Basin (consisting of the Taklamakan Desert and the adjacent mountains), including sample locations and sand roses with capacity of drifting for the 145-μm mean grain size population. RDD, resultant drift direction; VU, vector unit; Arm, proportional in length to amount of drifting sand from a given direction toward the white center circle; see Table 1 and section 3.3 for more details of sand roses.

proportion of sediments within the deserts, is important for understanding regional surface processes and local climatic and environmental evolution. The dust fraction interacts with the cycles of water, carbon, and energy and has a global significance by participating in a wide range of physical, chemical, and biogeological processes, such as the scattering of solar radiation, changing cloud properties, and affecting ocean biogeochemistry via its iron content (Goudie & Middleton, 2006; Jickells et al., 2005; Shao et al., 2011). However, because the dust fraction sometimes comprises only a small proportion of desert sediments, less attention has been paid to determining its provenance. In fact, many studies have assumed that both the sand and dust fractions have the same provenance, which has resulted in misinterpretations (Laceby et al., 2017). For example, Chen et al. (2007) showed that the <75-μm and <5-μm fractions of Chinese desert sediments have different Nd and Sr isotopic compositions. The consideration of whether different grain size fractions originated from separate source areas is crucial for resolving conflicts in the interpretation of the provenance of desert sediments. In addition, the scientific community is also discovering more and more that techniques commonly used to identify sediment source areas (not only for aeolian sediment or desert settings in particular, but anywhere) often turn out to be grain size dependent (Laceby et al., 2017), for example, mineralogy (Garzanti et al., 2009) and Nd-Sr isotopic composition (Jonell et al., 2018). The grain size dependence of these techniques also should be considered in resolving conflicts in the interpretation of sediment provenance.

The Taklamakan Desert (Figure 1) is an important source of global dust (Williams, 2014) and hosts the largest sand sea (~330,000 km^2 in area) in the midlatitudes (Goudie, 2013). Thus, sediment provenance of the desert is a key issue in understanding its aeolian system. The Taklamakan Desert is typical of deserts located in enclosed basins (which differs from the situation in tectonically stable desert regions in Africa, Australia, and the Arabian Peninsula; Lancaster, 1995), and of deserts located in rain shadow zones in midlatitudes (Goudie, 2002). Several studies have attempted to determine sediment sources of the Taklamakan Desert (Chang et al., 2000; Hattori et al., 2003; Honda & Shimizu, 1998; Rao et al., 2015; Rittner et al., 2016; Yang et al., 2007; Zhu et al., 1981). Although many valuable conclusions have been presented, there are still conflicting interpretations, mainly concerning the uniformity of the desert sediments, and the nature of the sediment contributions of the surrounding mountains. For example, Zhu et al. (1981) argued for a local origin of the sediments in all areas of the desert, based on heavy mineral assemblages. In addition, several studies have concluded from geochemical data that the aeolian sediments of the entire desert are homogeneous (Chang et al., 2000; Hattori et al., 2003; Honda & Shimizu, 1998). Rao et al. (2015) emphasized the contribution of the Tian Shan Mountains (Figure 1) in supplying sediment to the aeolian system of the desert, based on Nd-Sr isotopic composition. Rittner et al. (2016) argued that the Kunlun Mountains (Figure 1) are the main source of the desert sediments, based mainly on detrital zircon U-Pb ages and mineralogy. These contrasting interpretations can be attributed to specific grain size fractions having different source rocks (Laceby

et al., 2017). Yang et al. (2007) demonstrated the homogeneity of the fine fraction (<53 μm) and the significant differentiation of the coarse fractions (>250 μm) for the entire desert. This study suggested the possible usefulness of a grain-size-based approach for resolving a series of interpretational problems. Notably, this type of approach has seldom been used for studying the modern sediment supply mechanisms of the Taklamakan Desert. In addition, the importance of the Taklamakan Desert as a major dust source for the Chinese Loess Plateau has been controversial (Maher, 2016; Nie et al., 2015, 2018). In the present study, we address both issues: the modern sediment supply mechanisms of the Taklamakan Desert and the relative importance of silt-producing mechanisms for the desert dust.

Various techniques have been used to trace provenance of desert sediment. These include sediment composition using major, trace, and rare earth elements (REE; Chang et al., 2000; Honda & Shimizu, 1998; Hu & Yang, 2016; Liu & Yang, 2013, 2018; McLennan et al., 1993; Muhs, Bettis, et al., 2008; Muhs, Budahn, et al., 2008; Muhs et al., 2017; Muhs, 2017; Yang et al., 2007), isotopic composition (Chang et al., 2000; Hattori et al., 2003; McLennan et al., 1993; Rao et al., 2015), mineralogy (Honda & Shimizu, 1998; Lancaster et al., 2015; Muhs, Bettis, et al., 2008; Muhs, Budahn, et al., 2008; Muhs et al., 2017; Muhs, 2017; Rittner et al., 2016; Zhu et al., 1981), detrital zircon U-Pb ages (McLennan et al., 1993; Rittner et al., 2016), and grain size analysis (Honda & Shimizu, 1998; Lancaster et al., 2015; Langford et al., 2016; Muhs, Budahn, et al., 2008; Weltje & Prins, 2007). We collected a series of sediment samples along a north-south transect across the sand sea of the Taklamakan Desert for the measurement of the major, trace, and REE composition of the sand (>63 μm) and dust (<63 μm) fractions, with the aim of determining their respective provenances and to understand the modern supply mechanisms of the desert.

2. Regional Setting

The Tarim Basin, located in the center of the Eurasian Plate, is fringed by the Tian Shan Mountains, the Kunlun Mountains, and the Altun Mountains to the north, south, and southeast, respectively (Figure 1). The mountain ranges are >4.000 m a.s.l. (above sea level) and the basin floor elevation varies from approximately 780 to 1,500 m a.s.l. The Taklamakan Desert (~330,000 km^2 in area), ~500 km in width, and ~1,100 km in length, occupies the basin and is a sink for the sediment eroded from the surrounding mountains. The aridification of the basin and the formation of the Taklamakan Desert have resulted from the extreme distance to oceanic moisture sources and the development of topography which functioned as barriers to moisture transport (Goudie, 2002; Yang & Eitel, 2016; Zhu et al., 1981). The southwestern part of the basin is higher than the northeast; the lowest point of the basin, in the east, contains the former Lop Nor Lake (Zhu et al., 1981).

Some 85% of the Taklamakan Desert is occupied by active dunes, which cover an area of ~280,000 km^2 and comprise the largest sand sea in the midlatitudes of the Northern Hemisphere (Yang & Eitel, 2016; Zhu et al., 1981). The desert contains various types of dunes, some of which are more than 100-m high (Goudie, 2013; Zhu et al., 1981). The sediment budget of the desert is very positive (Goudie, 2013; Kao et al., 2001). This is due largely to the high degree of erosion, including both fluvial and glacial erosion in the surrounding mountains, in turn resulting from high relief, due to the rapid rate of uplift and the very large height difference (Goudie, 2013; Yang & Eitel, 2016). Water in the desert is mainly supplied by rivers originating from the surrounding mountains (Zhu et al., 1981).

In a tectonic framework, the Cenozoic Tarim Basin subsiding is linked to the overthrusting by the Tian Shan Mountains and the Kunlun-Altun Mountains in the north and the south of the basin, respectively (Allen et al., 1999; Jiang et al., 2004). According to the Atlas of Chinese geology (Ma et al., 2002), the basement rocks of the surrounding mountains are composed of granitic rocks from Proterozoic to Cretaceous ages and sedimentary rocks (chiefly limestone, shale, and sandstone) from Precambrian to Quaternary ages. Most of the Precambrian rocks in the surrounding mountains have been metamorphosed, and the area of unmetamorphic strata in the Tianshan Mountains is larger than that in the southern mountains (Ma et al., 2002). In addition, magmatic rocks of the Tianshan Mountains are mainly calc-alkaline series characterized by higher concentrations of CaO in relation to alkalines in comparison with alkaline igneous rocks, while those of the Kunlun Mountains and Altun Mountains are mainly alkaline series (Ma et al., 2002).

There are several drainage systems in the Tarim Basin (Yang, Liu, et al., 2006; Yu et al., 2016). Previously, nine drainage systems flowed into the mainstream of the Tarim River, the principal river in the basin

Table 1
Sand Transport Potentials of Meteorological Stations in and Around the Taklamakan Desert, Calculated Following Fryberger and Dean (1979), Based on the Average Annual Wind Energy Enabling Transport of Two Sand Populations (M_z = 300; 145 μm, Respectively)

				M_z = 300 μm				M_z = 145 μm			
Station Name	Latitude (°)	Longitude (°)	Elevation (m)	DP	RDP	RDP/DP	RDD	DP	RDP	RDP/DP	RDD
Alar	40.500	81.050	1013	9	7	0.74	185	27	17	0.63	191
Bachu	39.800	78.566	1117	8	6	0.86	220	26	19	0.73	218
Hotan	37.133	79.933	1375	2	1	0.84	92	14	8	0.59	91
Kashi	39.542	76.019	1380	92	87	0.94	143	166	146	0.88	144
Korla	41.733	85.816	903	46	43	0.94	226	108	93	0.87	228
Kuqa	41.716	82.950	1100	11	7	0.60	185	33	14	0.44	190
Pishan	37.616	78.283	1376	1	1	0.96	117	10	7	0.66	120
Ruoqiang	39.033	88.166	889	75	61	0.82	242	146	109	0.74	240
Shache	38.433	77.266	1232	6	5	0.97	126	17	14	0.82	131
Tazhong	39.000	83.666	1099	41	27	0.67	221	103	66	0.64	227
Tikanlik	40.633	87.700	847	49	46	0.95	253	96	85	0.88	255

Note. The wind energy for sand transport in desert environments is classified as follows: low energy, DP <200 VU; intermediate energy, DP 200–399 VU; high energy, DP >400 VU. Mz, mean grain size; DP, drift potential and is numerically expressed in vector unit (VU); RDP, resultant drift potential; RDP/DP, directional variability of the wind; RDD, resultant drift direction, listed as compass directions in degrees.

(Yang, Liu, et al., 2006; Yu et al., 2016); however, today only three drainage systems (the Aksu, Hotan, and Yarkant rivers) feed the main Tarim River. Currently, the Aksu River, which originates in the Tian Shan Mountains, contributes >70% of the total replenishment of the modern Tarim River (Ye et al., 2014). The runoff volumes of the rivers in the Tarim Basin are distinctly seasonal and vary positively with their sediment loads (Ye et al., 2014). In the flood season (June–September), ~75% of the annual runoff for the Tarim River carried ~95% of the annual sediment load (~25×10^6 tons), according to data from the Alar hydrological station (Ye et al., 2014). Infiltration and evaporation promote sediment deposition along the river channel (Langford, 1989). The fluvial channels are relatively mobile, which is a distinguishing feature of the entire fluvial system of the basin, because of the flat topography, channel aggradation, and abrupt fluctuations in runoff (Langford, 1989). Thus, the main channel of the Tarim River has a maximum width of 1–2 km, but the maximum width of the potential floodplain is ~100 km (Zhu et al., 1981). In the dry season, low river levels enable the floodplains to dry out, and the fluvial sediments are reworked by wind and are potentially supplied to the aeolian system (Langford, 1989).

The wind direction in the Tarim Basin is mainly controlled by topography (Gao & Washington, 2009; Goudie, 2013), and sand roses of data from meteorological stations (Figure 1) show that sand transport by wind is funneled from north to south. The modern Taklamakan Desert is geomorphologically active and there is sufficient wind energy to mobilize sediment; furthermore, it is one of the dustiest places on Earth, with the frequency of dust storms exceeding 50 days/year and the maximum yearly frequency of dust weather reaching >260 days/year (Maher, 2016; Qian et al., 2002). In contrast, using the Fryberger and Dean (1979) method, measured values of DP (drift potential) and RDP (resultant drift potential) are relatively low and indicate a low degree of drift potential for sand particles by wind (Table 1). It should be noted, however, that the apparent low DP is explained by the fact that the stations are located in artificial oases, surrounded by vegetation belts (Figure 1; Bruelheide et al., 2003; Okin, 2013).

3. Materials and Methods

3.1. Sampling

We hypothesized that sediment provenance in the Taklamakan Desert is likely to be a function of the nearly south-north orientation of the rivers and wind flows, and the east-west orientation of the surrounding mountain ranges (Figure 1). Therefore, we collected 30 samples along a south-north transect within the Tarim Basin, including 27 dune sediment samples and 3 fluvial sediment samples (Figure 1). The 27 aeolian dune sediment samples (from 0- to 5-cm depth and ~500 g in weight) were collected from the surface of active dune ridges during periods of minimal wind speed when there was no dust movement. Twenty-six desert sands (DS) samples were taken within the sand sea of the desert, and one TN sample from a dune

at the north side of the Tarim River. Most of the samples were collected along the highway from Minfeng to Luntai. All fluvial sediment samples (0- to 5-cm depth and ~1,000 g in weight) were collected from sand ripples of the surface of the valley floor, including two NR samples from the Niya River and one TR sample from the Tarim River. The sediments of the Niya River are mainly derived from the Kunlun Mountains and the sediments on the north side of the Tarim River mainly from the Tian Shan Mountains. We assume that samples NR01 and NR02 provide signatures of the Kunlun Mountains and that samples TR01 and TN01 provide signatures of the Tian Shan Mountains.

3.2. Grain Size Analysis and Sample Fractionation

Samples were oven-dried, and then 100 g of each sample were sieved for 20 min using sieves of 0.25φ intervals [$\varphi = -\log_2$ (grain diameter in mm)], with a shaking machine (Retsch AS200). Subsamples were weighed with an accuracy of 1 mg. All samples were separated into sand (>63 μm) and dust (<63 μm) fractions using a 63-μm mesh sieve. Grain size parameters (including mean, standard deviation, skewness, and kurtosis) were calculated using GRADISTAT (Blott & Pye, 2001), following Folk and Ward (1957). Sediment is generally the product of several processes, and thus the grain size distribution (GSD) often comprises more than one population (McTainsh et al., 2013). Parametric curve-fitting procedures can be used to decompose a GSD into genetically significant GSD populations, such as the end-member mixing analysis (EMMA) model of Weltje and Prins (2007), which has been implemented in MATLAB (Paterson & Heslop, 2015). The model was used successfully by Langford et al. (2016) to identify aeolian sediment provenance. Thus, the EMMA of grain size data was performed following Paterson and Heslop (2015), to obtain genetically meaningful interpretations of different grain size populations (Langford et al., 2016; Weltje & Prins, 2007).

3.3. Calculation of Sand Drift Potential

Sand drift potential was calculated from wind data obtained from the U.S. National Climatic Data Center during 1983–2012 from 10 meteorological stations on the periphery of the Taklamakan Desert and during 2003–2012 from the Tazhong meteorological station in the center of the desert (Figure 1). DP, RDP, RDD, and RDP/DP for all stations were calculated, using the method of Fryberger and Dean (1979), but with different values of the threshold wind velocity which were extrapolated to 10-m height ($V_{t(10m)}$). $V_{t(10m)}$ of the 300-μm mean grain size population is 596 cm/s (Fryberger & Dean, 1979), and $V_{t(10m)}$ of the 145-μm mean grain size population is 385 cm/s. $V_{t(10m)}$ of the 145-μm mean grain size population was obtained using data from Bagnold (1941) and Belly (1964) and calculated following Fryberger and Dean (1979). The equation is $V_{t(10m)} = 5.75V_t^* \log\frac{Z}{Z'} + V_t'$ (Fryberger & Dean, 1979), where V_t^*, Z, Z', and V_t' are 11.25 cm/s, 970 cm, 0.381 cm, and 164.592 cm/s, respectively (Bagnold, 1941; Belly, 1964).

3.4. Geochemical Analysis

The calcium carbonate content of the bulk and the two separated fractions were measured using the gasometric method. Dilute HCl (10%) was added to the samples and the volume of CO_2 released in a closed system under constant temperature, pressure, and with the absence of other gases, then measured with a volumetric calcimeter (Eijkelkamp). The measurement errors are 3 g/kg for carbonate content <50 and 6 g/kg for carbonate content in the range of 50–150 g/kg, 9 g/kg for carbonate content in the range of 150–180 g/kg, and less than ±5% of the average of two measured results for carbonate content >180 g/kg. The results (in mol/100 g) are listed in the supporting information.

The bulk and separated samples were also used for geochemical analysis. Samples were finely ground in an agate mortar grinder (Retsch RM200) and then used for measurements of major, trace, and REE. Major element contents of all powder samples were measured using an X-ray fluorescence spectrometer (XRF), PANalytical AXIOS, at the Institute of Geology and Geophysics, Chinese Academy of Sciences. The values are expressed as weight percentages (wt %). Loss-on-ignition (LOI) was determined by weighing samples after heating at 1000 °C for 1 hr. Analytical uncertainties are less than ±2% for all major elements except for MnO and P_2O_5 (up to ±5%). The chemical index of alteration (CIA) was calculated using the formula proposed by Nesbitt and Young (1982): $CIA = [Al_2O_3/(Al_2O_3+CaO^*+Na_2O+K_2O)] \times 100$ (ratio in molecular proportions), assuming that the amount of CaO^* is CaO only incorporated in silicates. Here, three CIA values, CIA, $CIA^{\#}$, and CIA^*, were calculated using different values of CaO^*. CIA was calculated using CaO^* by estimating CaO with correction by the calcium carbonate and apatite contents, following Nesbitt

and Young (1982); the calcium carbonate is measured by the gasometric method. $CIA^{\#}$ was calculated assuming $CaO^{*} = Na_2O$ (in moles), following McLennan (1993); and CIA^{*} was calculated using $CaO^{*} = 0.7Na_2O$ (in moles) by assuming a molar ratio of 1:3 for Ca:Na, following Honda and Shimizu (1998). In addition, the plagioclase index of alteration (PIA) was calculated following Fedo et al. (1995): $PIA = [(Al_2O_3 - K_2O)/(Al_2O_3 + CaO^{*} + Na_2O - K_2O)] \times 100$ (ratio in molecular proportions).

Measurements of the abundance of trace elements and REE were made on powder samples using an inductively coupled plasma-mass spectrometry (ICP-MS), NexION300D, in the Chinese Ministry for Nuclear Industries. The powder samples were pretreated by digestion with ultrapure acids under high temperature and pressure. To be specific, 40-mg sample powders, 1-ml HF, and 0.3-ml (1:1) HNO_3 were in a capped Teflon vessel, shaken for 15 min with an ultrasonic device and then heated for 24 hr on a ~120 °C hotplate. After that, the powders, 1-ml HF, 0.3-ml (1:1) HNO_3, and 0.5-ml $HClO_4$ were placed in a sealed Teflon vessel and heated for 7 days at ~120 °C. Two-milliliter (1:1) HNO_3 were further added and dried twice until no remaining residue was detectable. Finally, dissolved samples were diluted to 49 ml with 1-ml 1% HNO_3, and 500-ppb indium was added as internal standard. The analytical uncertainties (relative standard deviation) are less than ±1% for the REE and under ±5% for the trace elements. The chemical composition of the upper continental crust (UCC) is from Taylor and McLennan (2008). REE concentrations were normalized to chondrite compositions indicated by the "N" subscript, using values recommended in McLennan (1989). The Eu anomaly was quantified by Eu/Eu^{*}, where Eu is Eu_N, and $Eu^{*} = (Sm_N \times Gd_N)^{1/2}$ (Muhs, 2018; Taylor & McLennan, 1985).

4. Results

4.1. Grain Size

The variations of mean grain size, degree of sorting, and the content of the dust fraction (<63 μm) along the south-north transect are illustrated in Figure 2. The mean grain size ranges from 89–281 μm, the degree of sorting ranges from 1.29 (well sorted) to 2.33 (poorly sorted), and the content of the dust fraction ranges from 0.44–21.7%. The dominant grain size category of the samples is sand (Figure 2). The dust fraction content of the fluvial sediment samples, except NR02, is higher than that of dune sediment samples; in addition, from south to north, the mean grain size and sorting of the samples decrease rapidly, with a relatively smooth pattern of changes (Figure 2).

EMMA uses unbiased correlations of the grain size distributions of populations to identify the sources of grain size variations across sand seas (Weltje & Prins, 2007). Prior to EMMA, the variances of different numbers of end-members were assessed. The results are presented in Figure 3a, and they show that dividing the samples into three end-members is appropriate for the data set from the Taklamakan Desert. As shown in Figure 3b and Table S1, End-member 1 (EM1) represents a relatively fine component with a distribution which is well sorted, symmetrical, and platykurtic, with a mean grain size of 92 μm; End-member 2 (EM2) represents an intermediate component which is well sorted, fine skewed, and mesokurtic, with a mean grain size of 141 μm; and End-member 3 (EM3) represents a relatively coarse component which is moderately sorted, fine skewed, and leptokurtic, with a mean grain size of 261 μm. The samples dominated by EM1 are widely distributed within the entire Taklamakan Desert; those dominated by EM2 are located in the northern part of the desert; and those dominated by EM3 are located in the southern part of the desert (Figure 3c).

4.2. Major Elements

All samples are CaO-rich compared with UCC (Figure 4; Taylor & McLennan, 2008). Except for CaO, the bulk and sand fractions of the samples have a very similar weight percentage of SiO_2 and lower percentages of other major elements, compared with UCC (Figure 4). The dust fraction of the samples has varying weight percentages of Fe_2O_3, and higher TiO_2, MnO, MgO, and P_2O_5 and lower SiO_2, Al_2O_3, Na_2O, and K_2O, compared to UCC (Figure 4). In addition, the contents of SiO_2, Al_2O_3, Na_2O, and K_2O in the dust fraction are lower than those in the sand fraction, whereas the contents of other major elements are higher (Figure 4). Notably, samples NR01 and NR02 have a higher Fe_2O_3 content and lower CaO content than samples TN01 and TR01 (Figure 4).

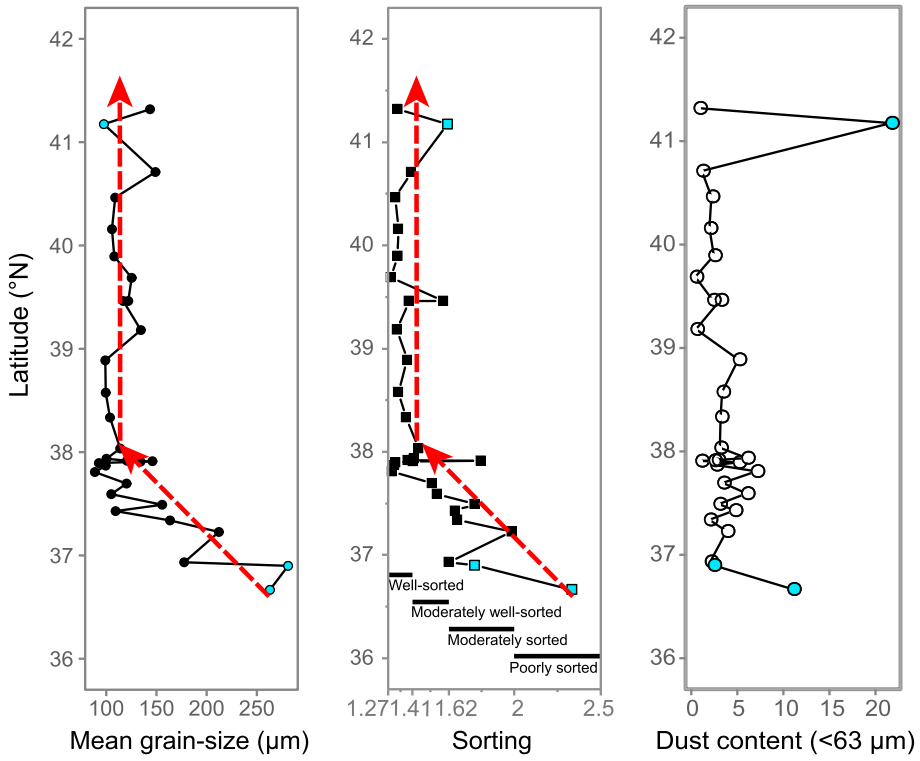

Figure 2. Variations of (left) mean grain size, (middle) sorting and (right) dust fraction content (<63 μm) with latitude. Blue color refers to the fluvial sediment samples.

A plot of Log (Na_2O/K_2O) versus Log (Si_2O/Al_2O_3) (Pettijohn et al., 1972) provides a dimensionless comparison of the plagioclase and quartz content of samples, irrespective of the calcium carbonate content (Muhs et al., 2013). Log (Na_2O/K_2O) is a measure of the proportion of plagioclase relative to K-feldspar, and Log (Si_2O/Al_2O_3) is a measure of the proportion of quartz relative to total feldspar (Pettijohn et al., 1972). As shown in Figure 5, most of the samples fall within the range of graywacke. The values of Log (Na_2O/K_2O) within the dust fraction group and bulk + sand fraction group of the desert sediment samples are relatively well grouped (Figure 5). In addition, most of the Log (Si_2O/Al_2O_3) values of the dust fraction (ranging from 0.75–0.80) are slightly lower than those of the sand fraction (ranging from 0.74–0.84).

4.3. Trace Elements

Most of the trace elements of the samples are depleted with respect to the UCC (Figure 6). The bulk and sand fractions of the samples have distribution patterns similar to the dust fraction, except for a higher content of

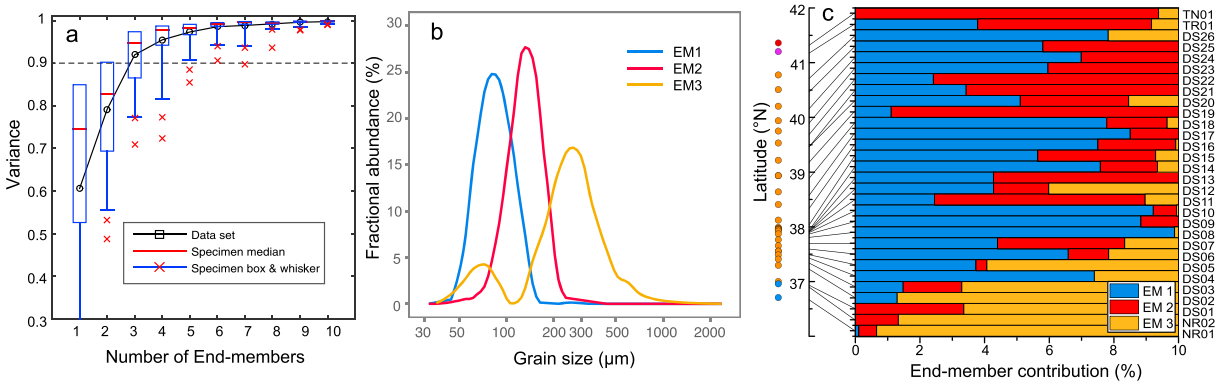

Figure 3. Boxplots of the percentage variance of samples explained by different numbers of end-members (a), indicating that three end-members are appropriate for this data set. Plot of the grain size distributions of the three end-members (b). Variation of end-member percentages with latitude (c).

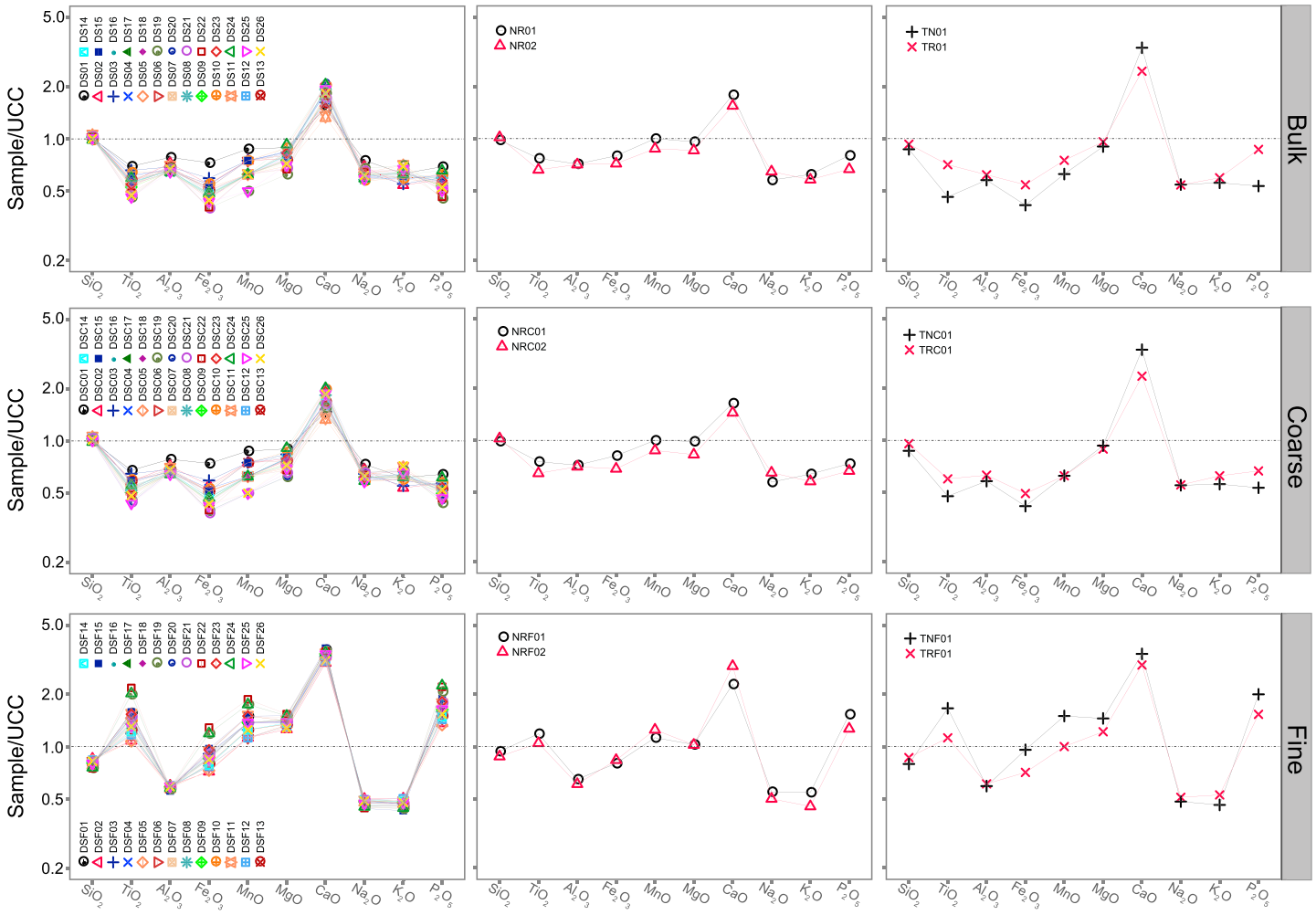

Figure 4. Upper continental crust-normalized major elemental patterns for bulk, sand, and dust fractions of the samples. (top row) Bulk indicates bulk samples, (middle row) Coarse (C) the sand fraction, and (bottom row) Fine (F) the dust fraction, respectively.

Rb, Mo, and Tl and a lower content of Y, Zr, Nb, In, Hf, W, Th, and U. Samples NR01, NR02, TN01, and TR01 have distribution patterns similar to those of the DS samples (Figure 6). In the bulk samples and sand fractions, the contents of Sc, V, Cr, Co, Ni, Cu, and Zn of samples NR01 and NR02 are higher than those of samples TN01 and TR01, whereas the dust fraction of samples NR01 and NR02 have higher values of Tl and lower values of W (Figure 6).

Selected trace element ratios can be used to identify distinctive components of samples which have important provenance and tectonic implications (McLennan et al., 1993); an example is Cr/V versus Y/Ni (Hiscott, 1984). Figure 7 shows a mixing curve which links an ultramafic end-member and a granite end-member, and it provides a semiquantitative estimate of the amount of ultramafic detritus in sediments (Amorosi et al., 2002). In this diagram (Figure 7), all the studied samples are much closer to the granite end-member than to the ultramafic end-member. The samples have Cr/V values <1.0 and Y/Ni values <0.50, with a <1% contribution of ultramafic detritus; by contrast, a >99% contribution occurs in granitic rocks. The range of Cr/V values of the dust fraction is similar to that of the sand fraction, whereas the range of Y/Ni values of the dust fraction is higher (Figure 7).

4.4. REE

The chondrite-normalized REE distribution patterns of all samples are characterized by relative enrichment of light REE [$(La/Sm)_N$ ranging from 3.23–4.73], a negative Eu anomaly (Eu/Eu^* 0.32–0.85), and a flat heavy

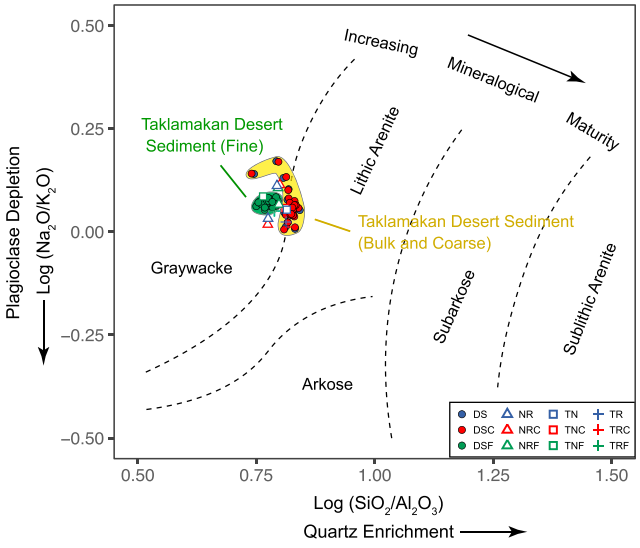

Figure 5. Plot of Log (Na_2O/K_2O) versus Log (Si_2O/Al_2O_3) for bulk, sand, and dust fractions of the samples, following Pettijohn et al. (1972). The values reflect mineralogical maturity. Bulk indicates bulk samples, Coarse (C), the sand fraction, and Fine (F), the dust fraction, respectively.

REE portion of the curve [$(Gd/Yb)_N$ 1.34–2.38; Figure 8]. Overall, the values are very similar to those of UCC (Figure 8; McLennan, 1989). The distribution in Figure 9a reveals an inverse correlation between Eu/Eu^* and ∑REE. The dust fractions have higher ∑REE (>160 ppm), higher heavy REE [most values of $(Gd/Yb)_N$ are >1.60], and more negative Eu anomaly values (values of Eu/Eu^* are <0.60) compared to the sand fraction (Figures 8 and 9).

A negative Eu anomaly (expressed as $Eu/Eu^* < 1.0$) results from incorporation of Eu in Ca-plagioclase, where Eu substitutes for Sr, which substitutes for Ca (Mason & Moore, 1982), and differences in the Eu/Eu^* values of aeolian sediments reflect differences in provenance (Liu & Yang, 2013, 2018; Muhs, Budahn, et al., 2008; Muhs, 2018). The Eu/Eu^* values of the dust fraction range from 0.32–0.56, which is lower than those of the sand fraction (0.64–0.83; Figure 8). In the sand fraction (Figures 8 and 9a), most of the Eu/Eu^* values of the desert dune sediments (0.67–0.83) are closer to those of samples NR01 and NR02 (0.71–0.79) than those of samples TN01 and TR01 (0.64–0.66). However, in the dust fraction (Figures 8 and 9a), many of the Eu/Eu^* values of the desert sediment samples are close to both of these groups of samples, and several Eu/Eu^* values are closer to those of samples TN01 and TR01 (0.42–0.49) than those of samples NR01 and NR02 (0.49–0.56).

5. Discussion

5.1. Feasibility of the Use of Chemical Composition for Determining Provenance

The chemical composition of clastic sediments is the combined result of the source rock composition and chemical weathering processes (Perri et al., 2013; Sawyer, 1986). Nesbitt et al. (1996) demonstrate that the chemical composition of mobile elements of sediments may not reflect provenance directly because of the effects of chemical weathering. Caracciolo et al. (2011) noted that potential provenance signatures indicated by chemical composition of mobile elements were overwhelmed by the strong effects of weathering processes in the Bohemian Cretaceous Basin. Hence, for identifying provenance of the Taklamakan Desert sediment by chemical composition of mobile elements, it is necessary to first evaluate whether the effects of chemical weathering processes have obscured potential provenance signatures.

The most widely used chemical indicator to detect the effects of the chemical weathering of sediments is the CIA, which was proposed by Nesbitt and Young (1982). The CIA values of fresh basalts (30–45) indicate the near absence of weathering (Nesbitt & Young, 1982), and the values of typical loess deposits (55–70) indicate moderate weathering (Taylor & McLennan, 1985). The range of CIA values of the bulk samples studied herein (45.2–56.2) is very similar to that of granites and granodiorites, higher than that of fresh basalts, and lower than that of loess (Figure 10). This indicates that the effects of chemical weathering on the desert sediment samples are minor. The degree of chemical weathering can also be estimated using the PIA, following Fedo et al. (1995). The PIA values of the bulk samples are relatively low, ranging from 43.9–57.9 (Figure 10), which indicates that only a small proportion of the plagioclase has been converted. Overall, therefore, the CIA and PIA values of the desert sediments indicate a low degree of chemical weathering.

The chemical composition of sediments changes through three principal processes: weathering of the source rocks, sorting, and, in some cases, recycling (Perri et al., 2013; Sawyer, 1986). Weathering of the source rocks typically occurs in the source area through pedogenesis and diagenesis and less frequently during subsequent transportation (Sawyer, 1986). Sorting is a mechanical process which occurs during sediment transport (Perri et al., 2013); it may result in the separation of coarse and fine particles or heavy and lighter minerals, and thus change the chemical composition of particle mixture. Garzanti et al. (2012) demonstrated that in at least some dryland areas, natural sorting processes do not overwhelm provenance signatures, even during long-distance transport. The effect of recycling on sediment chemical composition is element mobility during diagenesis and metamorphism (Sawyer, 1986). Results of weathering indices (CIA and PIA) reflect the sum of the effects, including weathering of the source rocks, sorting, and recycling. Thus, the

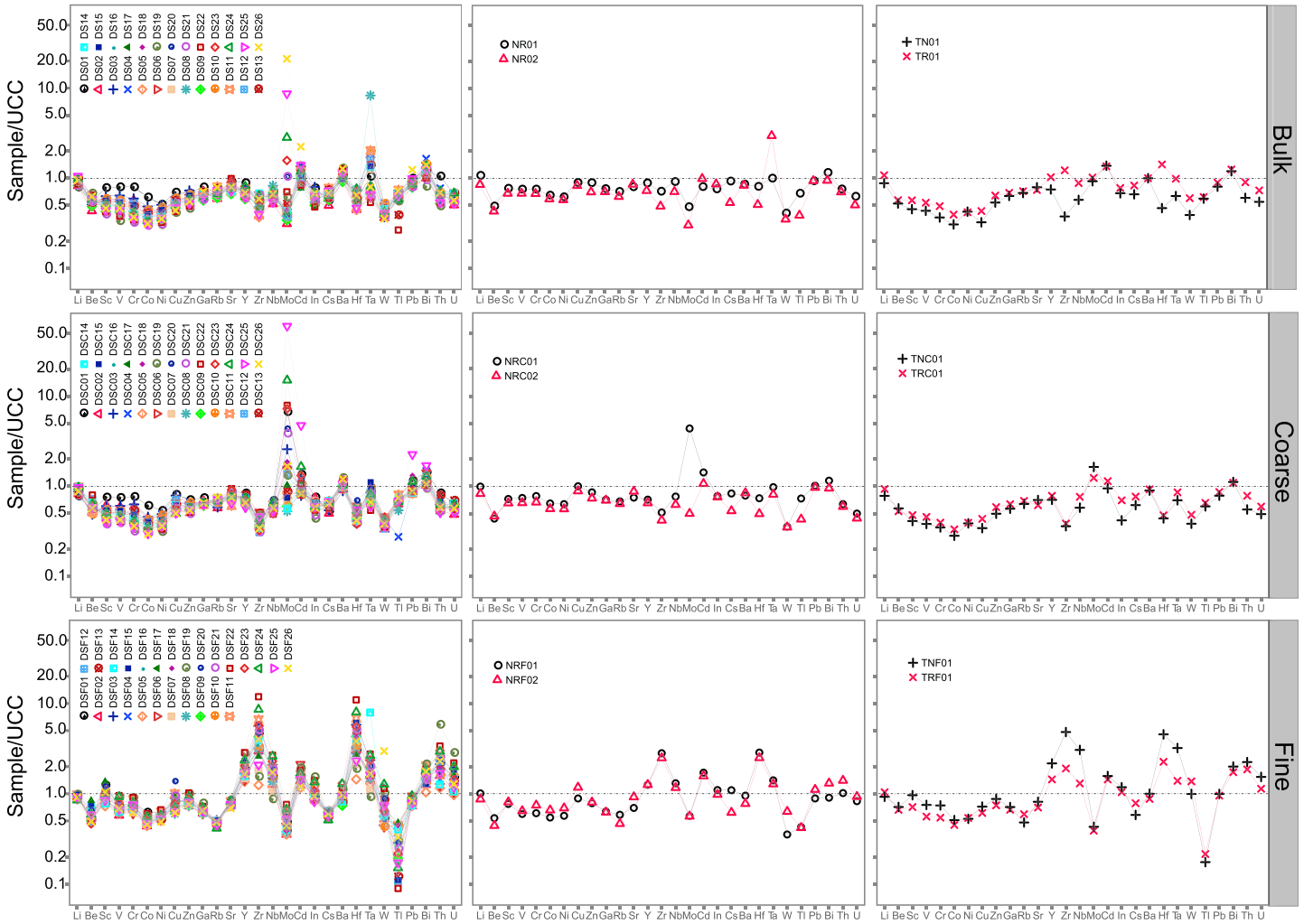

Figure 6. Upper continental crust-normalized trace element patterns of bulk and sand and dust fractions. (top row) Bulk indicates bulk samples, (middle row) Coarse (C), the sand fraction, and (bottom row) Fine (F), the dust fraction, respectively.

low values of the weathering indices (Figure 10) set a low upper limit on the effects. Hence, we consider that these processes have a very limited cumulative effect on the chemical composition of the desert sediments and that the provenance signatures of their chemical composition are largely unaffected, enabling them to be used for provenance analysis in the Taklamakan Desert. It is worth mentioning that if there were chemical weathering, geochemistry for provenance studies can still be used as long as only immobile elements are used.

5.2. Differences in the Provenances of the Sand and Dust Fractions

Chemical weathering can generate clay minerals from plagioclase, K-feldspar, and other minerals (e.g., pyroxenes, amphiboles, and micas; Nesbitt & Young, 1982); most clay minerals are fine grained (<2 μm) and are concentrated in the dust fraction (Nesbitt et al., 1996). The range of CIA values of residual clays (kaolinites and chlorites) mostly is 85–100, which indicates strong weathering (Taylor & McLennan, 1985). In general, the CIA values of most sediments are lower than those of clays, and chemical weathering tends to increase the CIA value of the dust fraction. If the sand and dust fractions of sediments are derived from the same source, weathering processes could cause the dust fraction to have a higher CIA value than the sand fraction. The main reason that dust might experience more chemical weathering is that its surface area/mass ratio is much greater than for sand, and it is likely to be more chemically active because of greater water-holding capacity. The CIA values of all fractions of the Taklamakan Desert samples (47.6–56.3; Figure 11) are much lower than those of kaolinites and chlorites (85–100). However, the range of CIA values of the dust fraction

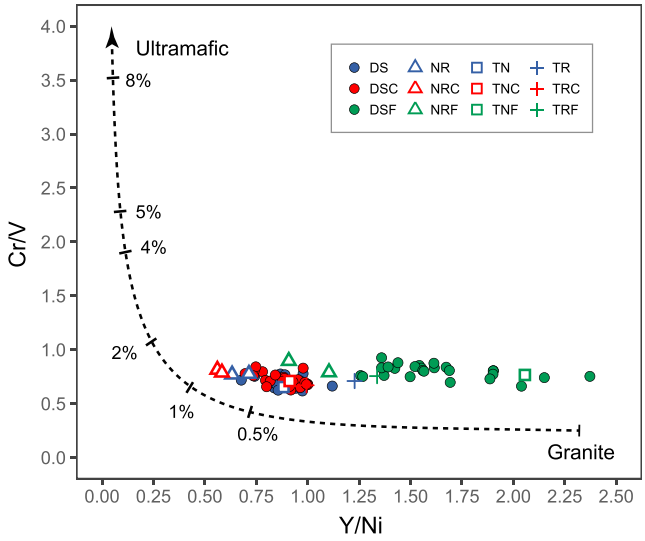

Figure 7. Plot of Cr/V versus Y/Ni for bulk and sand and dust fractions. The mixing curve, connecting a granite end-member to an ultramafic end-member, follows Amorosi et al. (2002). The percentages listed in the plot are percentages of an ultramafic component in the samples. Bulk indicates bulk samples, Coarse (C), the sand fraction, and Fine (F), the dust fraction.

(47.6–51.7) is lower than that of the sand fraction (51.1–56.3; Figure 11). This indicates that the sand and dust fractions of the desert sediments likely have different provenances.

Provenance signatures may be obscured by estimating the CaO^* content in the calculation of CIA in provenance research of desert sediments. Estimation of the CaO^* content is often used in the calculation of CIA values (e.g., Honda & Shimizu, 1998; Liu & Yang, 2018; Yang et al., 2007). $CIA^\#$ and CIA^* are calculated using two different methods: $CIA^\#$ uses a higher CaO^* content in the calculation than does CIA^* by assuming a higher ratio of Ca to Na (Honda & Shimizu, 1998; McLennan, 1993). The ranges of $CIA^\#$ values of all fractions of the desert sediments are lower than those of CIA^* (Figure 11), which is expected from the higher CaO^* content in the index calculation formula (section 3.4; Nesbitt & Young, 1982). The ranges of the values of CIA^* and $CIA^\#$ of the dust fraction are higher than those of the sand fraction, whereas the reverse is the case for the CIA (Figure 11). This implies a higher molar ratio of Ca to Na in the dust fraction than in the sand fraction. As shown in mineral data (Table S2), in the bulk, the dolostone ($CaMg(CO_3)_2$) contents of the desert dune sediments (2.1%) and the sediments from the southern rivers (1.5%) are much less than that of the northern rivers (9.0%). Dolostone, a sedimentary carbonate rock, is hard to react with dilute HCl (10%), and the dolostone content of samples cannot be measured using the gasometric method. As a result, the CIA values, calculated using CaO^* by estimating CaO with correction by the calcium carbonate which is measured by the gasometric method, are underestimated but can contain the provenance signature about dolostone, while the $CIA^\#$ and CIA^* values cannot. Thus, maybe the range of CIA^* values of the bulk samples studied herein (51.3–56.2) is closer to the true value range than the range of CIA values (45.2–56.2; Figure 11). The range of CIA^* values, same as the range of CIA values, also indicates a low degree of chemical weathering of the desert sediments. However, the information about dolostone is likely obscured by estimating the CaO^* content in the calculation of CIA, indicating that caution is needed when using the estimation in provenance research of desert sediments with potential source having dolostone.

Weathering processes produce clay minerals from primary minerals (Mason & Moore, 1982). Clay minerals are more Al-rich than plagioclase, K-feldspar, and quartz (Nesbitt & Young, 1982). Nesbitt et al. (1996) showed that different-sized particles with the same felsic provenance will exhibit a specific weathering trend as they evolve from sand to mud: from the CN-K [(CaO^*+Na_2O)-K_2O] side toward the A (Al_2O_3) apex in the ternary plot of A-CN-K (Figure 12a). Because CaO and Na_2O are lost to solution in the chemical weathering process, Al_2O_3, being far less soluble, stays close to the site of release after alteration of primary aluminosilicate mineral weathering (Mason & Moore, 1982). In addition, a specific weathering trend is expected in the ternary plot of (A-K)-C-N (Figure 12b; Fedo et al., 1995). During the same weathering process, La, Th, and Sc will be enriched, as these are relatively insoluble elements; there should not be a weathering trend in the ternary plot of La-Th-Sc. Figure 7 shows that the samples have Cr/V < 1.0 and Y/Ni < 0.50, with a <1% contribution of ultramafic detritus and a >99% contribution from granitic rocks (Amorosi et al., 2002). This indicates that the desert sediments have a felsic-dominated source and that specific trends can be expected if the sand and dust fractions have the same provenance. The weathering trends of the sand and dust fractions of the Taklamakan Desert sediment samples were examined using ternary plots (Figure 12). The grain size data (Figure 2) for the samples show that all the desert dune sediments have a dust fraction of <10%. As a result, the chemical signatures of the bulk samples are very similar to those of the sand fraction, and therefore, the two groups of samples were aggregated into a single group. The plots (Figure 12), however, exhibit reversed trends from the sand fraction to the dust fraction for specific weathering trends expected in the ternary plots of A-CN-K and A-CN-K, and exhibit an unexpected weathering trend from the sand fraction to the dust fraction in the ternary plot of La-Th-Sc. These reversed and unexpected trends indicate differences in provenance of the sand and dust fractions; moreover, the reversed and unexpected trends confirm that the chemical composition of the desert sediments can be used to reveal their provenance signatures.

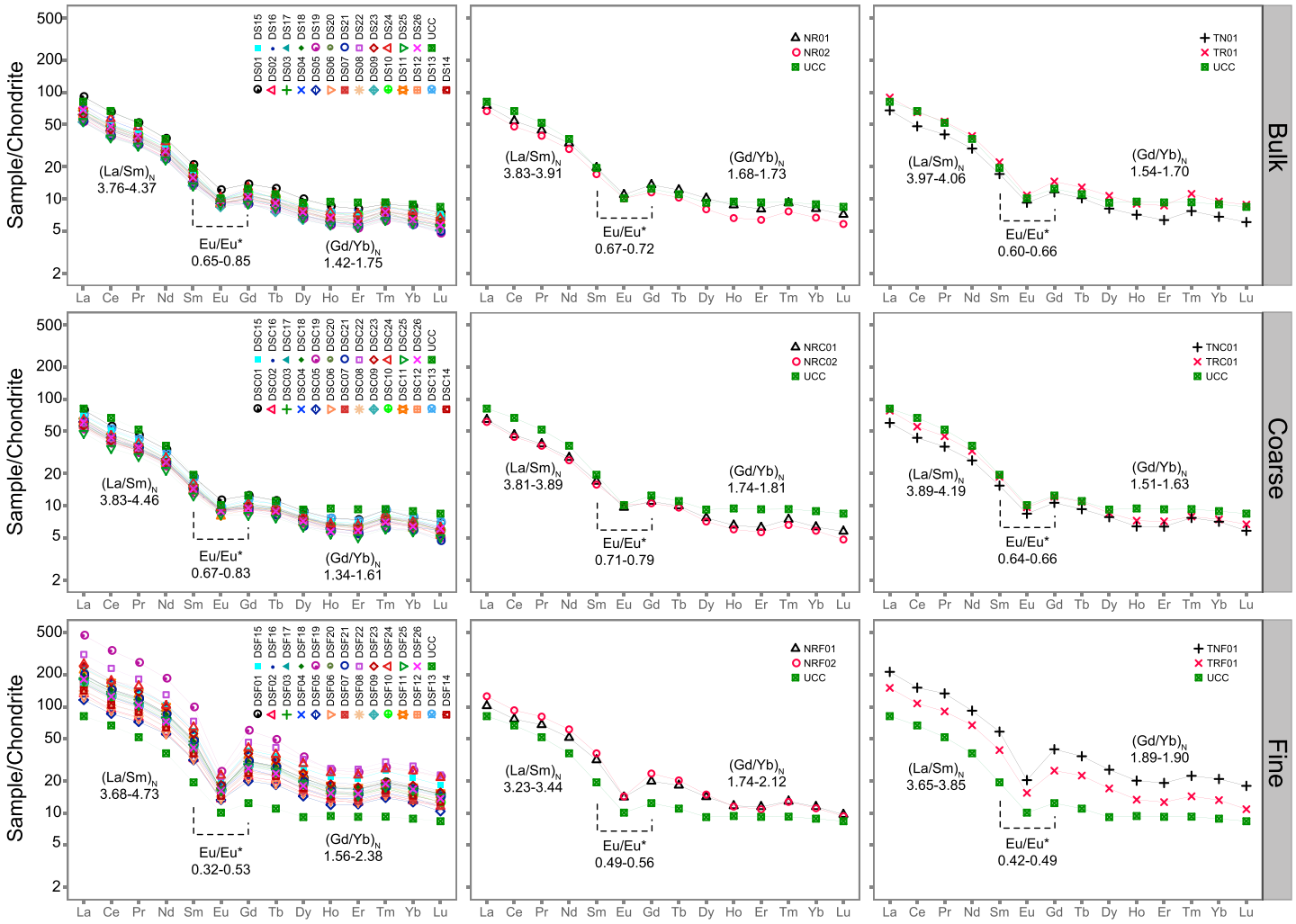

Figure 8. Chondrite-normalized rare earth elements patterns for bulk and sand and dust fractions. Bulk indicates bulk samples, Coarse (C), the sand fraction, and Fine (F), the dust fraction, respectively.

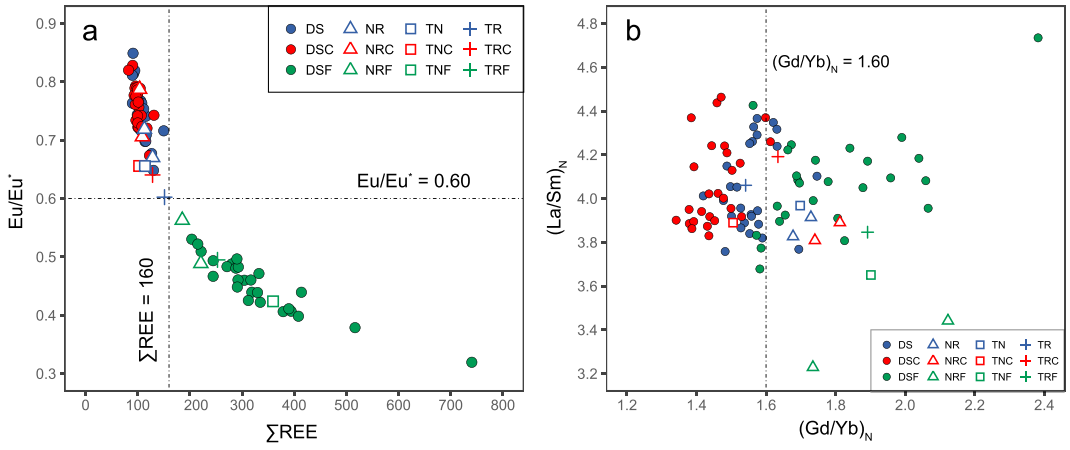

Figure 9. Plots of Eu/Eu^{*} versus $\sum REE$ (a) and $(La/Sm)_N$ versus $(Gd/Yb)_N$ (b) for bulk and sand and dust fractions. Bulk indicates bulk samples, Coarse (C), the sand fraction, and Fine (F), the dust fraction, respectively. REE = rare earth elements.

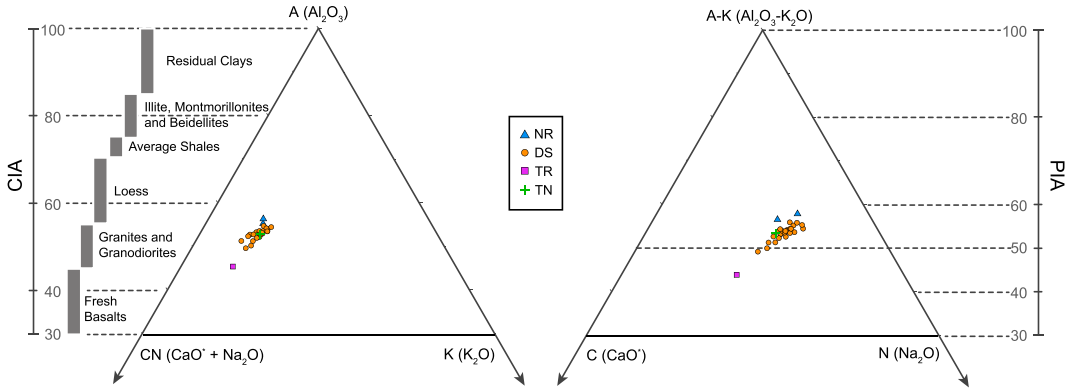

Figure 10. Ternary plots of A-CN-K with CIA and (A-K)-C-N with PIA of the bulk samples. The CIA values of fresh basalts, granites, and granodiorites are from Nesbitt and Young (1982); the CIA values of loess, average shales, illites, montmorillonites, beidellites, and residual clays (kaolinites and chlorites) are from Taylor and McLennan (1985). CIA = chemical index of alteration; PIA = plagioclase index of alteration.

5.3. Provenance of the Sand and Dust Fractions

Previous studies have emphasized the Kunlun and Tian Shan Mountains as major sediment sources for the Taklamakan Desert (Chang et al., 2000; Hattori et al., 2003; Rao et al., 2015; Rittner et al., 2016), and most controversy concerns the relative importance of these two sources. The sediment supply from the Altun Mountains to the desert is minor, although it cannot be excluded (Rao et al., 2015). Rittner et al. (2016) define a "Kunlun" group which includes the Kunlun and Altun Mountains. In the present study, following Rittner et al. (2016), we define the mountains surrounding the southern part of the Tarim Basin as the broader Kunlun Mountains.

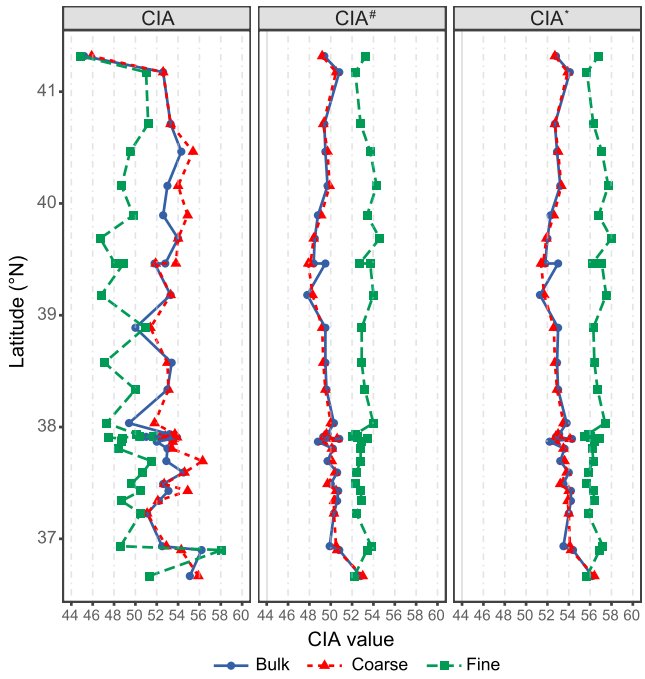

Figure 11. Variation of CIA, $CIA^{\#}$, and CIA^{*} with latitude for bulk, sand, and dust fractions of the Taklamakan Desert samples. CIA is calculated using CaO^{*} by estimating CaO with correction by the calcium carbonate and apatite contents, following Nesbitt and Young (1982); the calcium carbonate is measured by the gasometric method. $CIA^{\#}$ uses $CaO^{*} = Na_2O$ (in moles) by assuming a ~1:2 molar ratio of Ca: Na, following McLennan (1993). CIA^{*} uses $CaO^{*} = 0.7Na_2O$ (in moles) by assuming a ~1:3 molar ratio of Ca: Na, following Honda and Shimizu (1998). Bulk indicates bulk samples, Coarse (C), the sand fraction, and Fine (F), the dust fraction, respectively.

Generally, the values of sorting and mean grain size of sand-sized aeolian sediments decrease downwind (Lancaster et al., 2015), because wind preferentially removes the fine sand fraction of sediments by saltation, leaving a residue of larger particles (McTainsh et al., 2013). Traditional approaches have used grain size and sorting studies to constrain the provenance of the sand fraction of desert sediments in many different areas (Lancaster et al., 2015; Lancaster & Ollier, 1983). Figure 2 illustrates south-north trends of the mean grain size and sorting of the sediment samples. These trends suggest that the Kunlun Mountains, and not the Tian Shan Mountains, are the main source of the sand fraction of the Taklamakan Desert dune sediments.

The EMMA results for the Taklamakan Desert sediments (Figure 3 and Table S1) show that EM1 is the finest genetically significant population. The samples dominated by EM1 are distributed throughout the entire desert in a south-north direction (Figure 3c). This suggests that both the Kunlun and Tian Shan Mountains could be the potential provenances of the dust fraction of the desert sediments.

Eu is especially significant for tracing sediment provenance because it is the only element among the REEs that can exist stably in a divalent state (Mason & Moore, 1982). A negative Eu anomaly (measured by Eu/Eu^{*} which is a value less than 1.0) results from incorporation of Eu in Ca-plagioclase (Mason & Moore, 1982); it is a widely used index for tracing sediment provenance (Hu & Yang, 2016; Liu & Yang, 2013, 2018; Muhs, Budahn, et al., 2008; Muhs, 2018). Rb substitutes for K in the major rock-forming minerals, based upon the principles of element substitution (Mason & Moore, 1982). K/Rb can be used as a provenance tracing index

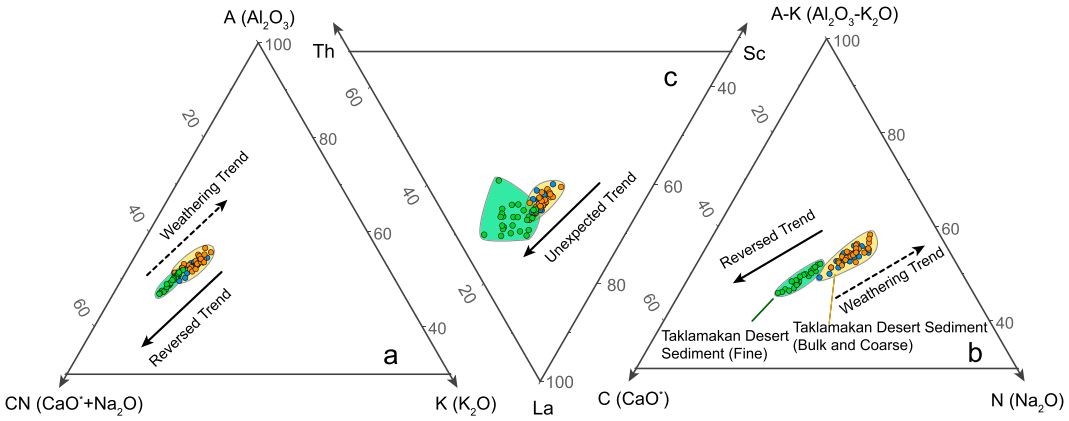

Figure 12. Ternary plots of A-CN-K (a), (A-K)-C-N (b), and La-Th-Sc (c) of bulk samples (yellow), and sand (blue) and dust (green) fractions of the desert dune samples. Dashed lines are weathering trends for sediments from the same provenance, and solid lines are reversed and unexpected trends caused by compositional variations owing to differences in provenance.

given its variability within different rock types (Muhs, 2017) and is well established in sedimentary research (Muhs, Bettis, et al., 2008; Muhs et al., 2017; Muhs, 2017). K/Rb was used to distinguish loess deposits of different provenance in Nebraska in North America (Muhs, Bettis, et al., 2008), and in addition it was used to distinguish aeolian sands of different provenance in the dune fields and sand seas of North America (Muhs, 2017; Muhs et al., 2017). Moreover, Muhs et al. (2017) proposed that K/Rb could be used as a provenance indicator in many sand seas worldwide.

Based on the aforementioned principles, Eu/Eu* and K/Rb were also used to identify the provenances of the sand and dust fractions of the Taklamakan Desert sediments (Figure 13). Since the dominant size class of the samples is sand (Figure 2), the chemical signatures of the bulk samples largely reflect the chemical signatures of the sand fraction. The signatures of the bulk and the sand fraction of the DS samples are very similar to those of the Kunlun-derived sediments; the Tian Shan-derived sediment samples have lower Eu/Eu* and K/Rb values than the other group (Figure 13). This finding reinforces the conclusion that the sand fraction of the desert sediments is mainly derived from the Kunlun Mountains, rather than from the Tian Shan Mountains. The dust fraction (Figure 13) has similarities to both the Kunlun-derived and the Tian Shan-derived sediment samples, despite the fact that their Eu/Eu* and K/Rb ratios are different. This reinforces the conclusion that dust fraction of the desert sediments is derived from both the Kunlun and the Tian Shan Mountains.

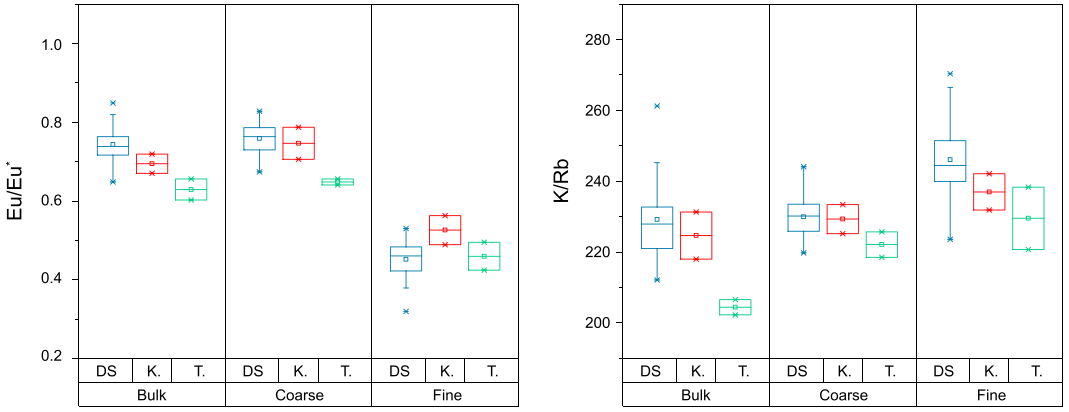

Figure 13. Boxplots of (left) Eu/Eu* and (right) K/Rb values for the sediment samples. DS = desert dune sediment samples; K. = Kunlun-derived fluvial sediment samples, including NR01 and NR02; T. = Tian Shan-derived samples, including TR01 and TN01. Bulk indicates bulk samples, Coarse (C), the sand fraction, and Fine (F), the dust fraction, respectively.

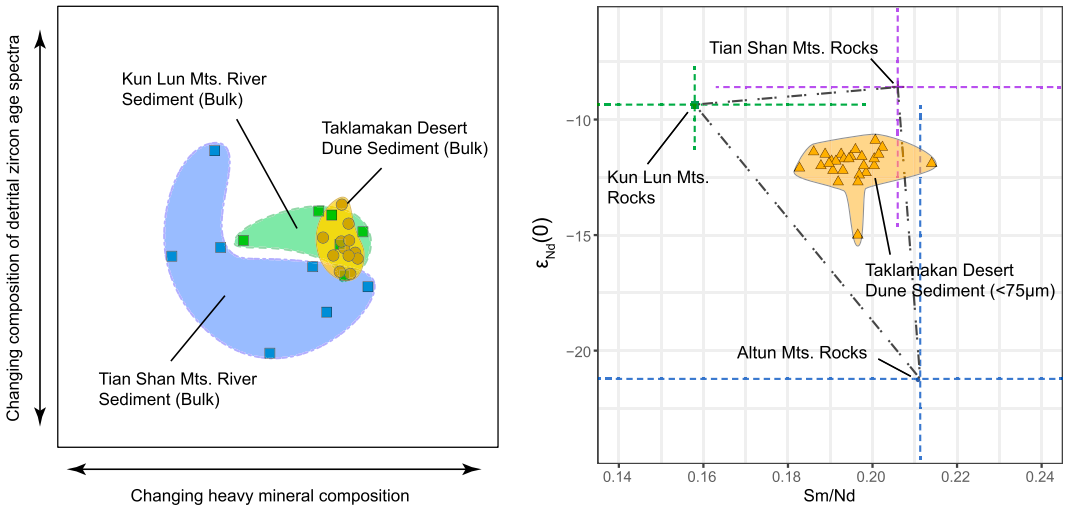

Figure 14. INDSCAL (Individual Differences Scaling) map (left) combining detrital zircon age spectra and heavy mineral composition of all dune and fluvial sediment samples in the Tarim Basin. Piedmont samples are excluded from the provenance sample group due to the likelihood that they comprise mixtures of many exogenous materials in the downwind part of the desert (modified after Rittner et al., 2016). Isotopic plot of $\varepsilon_{Nd}(0)$ versus Sm/Nd (right) of the fine fraction (<75 μm) of the Taklamakan Desert sediment samples (modified after Rao et al., 2015).

Although previous studies have presented valuable opinions on the provenance of the Taklamakan Desert sediments, there is still a lack of arguments for the differences in the provenances of the sand and dust fractions. Moreover, the previous studies could be controversial, as they were based on the assumption that the two fractions have the same source or without considering the grain size dependence of these techniques used to identify the provenance of the desert sediments. We propose that the controversies regarding the provenance of the desert sediments can be resolved by taking grain size effects into consideration. Our earlier studies found out that coarse sands show distinct variations from region to region but fine sands are quite homogeneous in the Taklamakan Desert (Yang et al., 2007). Rittner et al. (2016) showed that a group of bulk desert dune samples were very similar to a group of Kunlun-derived river sediment samples, based on detrital zircon age spectra and heavy mineral compositions, whereas they were dissimilar to a group of Tian Shan-derived samples (Figure 14, left). Desert sediments are dominated by sand-sized grains and the methodologies of both heavy mineral and zircon analyses exhibit a grain size bias which emphasizes sand grains rather than the dust fraction (Jackson et al., 2004). Thus, Rittner et al. (2016) came to the conclusion that the sands of the Taklamakan were mainly derived from the Kunlun Mountains. By contrast, Rao et al. (2015) showed that the sediments of this desert were closer to the end-member of rocks from the Tian Shan Mountains in an isotopic plot of εNd(0) versus Sm/Nd (Figure 14, right).

Our new data and the studies by Jonell et al. (2018) suggested that changes of isotopic compositions must be interpreted with consideration of chemical fraction of minerals in different grain size fractions. In this context, there are two potential explanations for the difference between the conclusions from Rittner et al. (2016) and Rao et al. (2015). One is that the bulk samples measured by Rittner et al. (2016) and the fine fractions measured by Rao et al. (2015) had different provenances, as they claimed. And the other is that the bulk samples and dust fractions might originate from the same provenance, and their different interpretations were actually due to the differences in selection of grain size fractions of samples for measurements. As Jonell et al. (2018) emphasized, certain minerals tend to end up in different grain size fractions, and the chemical fractionation by mineralogy may affect the inferred provenance signal even if the minerals in the fine sediment fraction were derived from the same source rocks as the minerals in the bulk samples. For a truly correct understanding geochemical data must be interpreted with consideration to the impact of grain size, and to the geomorphological processes and associated sediment supply mechanisms.

5.4. Sediment Supply and Availability

The sediment samples were collected from the surface; in addition, the geochemical tracers we use herein to identify desert sediment provenance have a temporal scale of $<10^4$ years in terms of sediment transport

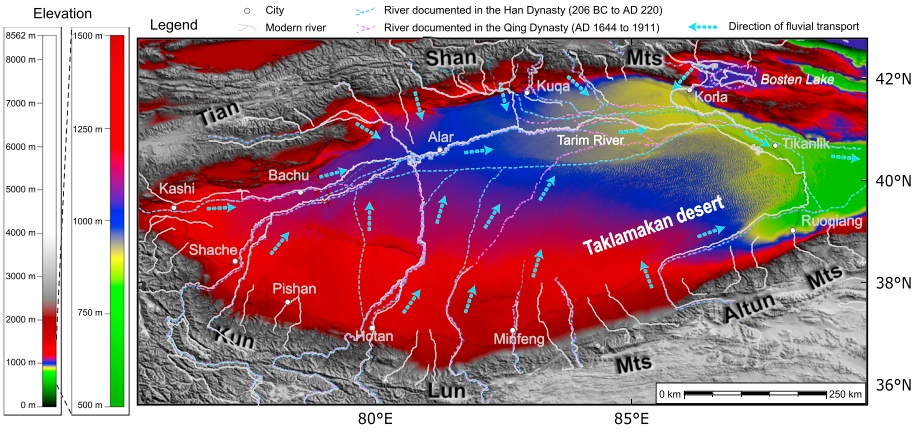

Figure 15. Elevation map of the Tarim Basin based on Shuttle Radar Topography Mission data (USGS, 2004) with historically documented rivers. The rivers of the Qing Dynasty are from Yang, Liu, et al. (2006), and those of the Han Dynasty are from Yu et al. (2016).

(Lancaster et al., 2013). Hence, we now try to determine the contemporary sediment supply mechanisms based on the provenance information. The formation and accumulation of sand seas are governed by sediment supply, availability, and wind power (Kocurek & Lancaster, 1999; Lancaster, 2013). The Taklamakan is currently an active desert, and there is sufficient wind energy to generate sediment mobility (Zhu et al., 1981). In addition, sediment supply is not a limiting factor for sediment accumulation, because ample sediment is still being generated in the adjacent mountain ranges (Goudie, 2013; Kao et al., 2001). Hence, to determine the contemporary sediment supply mechanisms from the provenance, the main factors to consider are the spatial characteristics of sediment supply and sediment availability.

Elevation is the major control on the spatial distribution of the rivers influencing the sediment supply of the Taklamakan Desert. Figure 15 shows that almost the entire desert can be regarded as a potential drainage area for the Kunlun-derived rivers, based on the gradient characteristics of the drainage basin elevation. The drainage systems of the desert exhibit a high degree of spatial variability (Figure 15; Yang, Liu, et al., 2006; Yu et al., 2016) and enable the direct supply of sediment to each part of their respective drainage areas. Furthermore, part of the Yarkant River and the Tarim River are located in the northern fringe of the desert at the lowest elevation of the north-south direction of the Tarim basin and are oriented in a west-east direction (Figures 1 and 15). The Yarkant-Tarim channel is a physical barrier for the smaller rivers carrying Tian Shan-derived sediment southward to the desert, and it transports sediment eastward along the desert fringe. Thus, since the development of the fluvial systems, the Kunlun Mountains have directly supplied sediment to the desert via fluvial processes; in contrast, this was not possible for the Tian Shan Mountains.

Vegetation provides a major control on the availability of sand particles for aeolian transport in the Tarim Basin. Vegetation reduces wind speed and thus decreases the aeolian transport of sediment (Draut et al., 2012; Li et al., 2013; Okin, 2013; Wolfe & Nickling, 1993; Zhu et al., 1981). Table 1 reveals the low drift potential of the sand particles in the oases of the basin, and it implies that the sand is anchored by the surrounding belts of vegetation. The Enhanced Vegetation Index (EVI) map (Figure S1) provides a consistent spatial comparison of the vegetation conditions in the basin (Didan, 2015). Minimal vegetation cover occurs along the Kunlun-derived rivers, especially for the segments in the center of the desert. In addition, the vegetation along the historically documented rivers (Figure 15) has evidently disappeared. Ye et al. (2014) showed that the runoff volumes of the rivers in the basin have a high seasonality and they vary synchronously with their sediment loads. The Kunlun-derived rivers supply abundant sand grains to the southern part, the center, and even the northern part of the desert, during the flood season. In addition, the Kunlun-derived sand particles are available for supply to the aeolian system within the desert when the rivers dry up and the vegetation disappears. It is for this reason that the sand fraction of the desert sediments mainly has the provenance signature of the Kunlun Mountains (section 5.3).

In the case of the Taklamakan Desert, the contemporary sediment supply mechanism of the dust fraction is more complex than that for the sand fraction. Gao and Washington (2009) studied the spatial characteristics

of dust activity over the basin, using TOMS AI (Total Ozone Mapping Spectrometer Aerosol Index) for 1980–1992. The results revealed dust hot spots in the basin (Figure S1) which were associated with intense dust activity near the surface. A hot spot is found in the southern part of the basin where abundant Kunlun-derived sediments accumulate. These sediments are transported northward to the desert by wind, but the amount transported is relatively low due to the low frequency of southerly winds (Figure 1). Nonetheless, some of the Kunlun-derived rivers directly supply dust particles to the center of the basin, whereas the Tian Shan-derived rivers do not. When the rivers dry up, the particles are available for aeolian transport due to the absence of vegetation. In addition, aeolian abrasion, a ubiquitous process within the desert, can generate some dust particles which inherit the provenance signature of the Kunlun Mountains in the desert sands.

There is also a dust hot spot in the northern part of the Tarim Basin. It includes the wide oases near the southern slopes of the Tian Shan Mountains (Figure S1), which have accumulated abundant Tian Shan-derived sediments. Although vegetation protects sediment from aeolian erosion, it also has the ability to trap windblown dust particles (Okin, 2013; Wolfe & Nickling, 1993); therefore, the dust fraction increases in the oases. Although vegetation does not eliminate entirely the aeolian transport of sediment (Okin, 2013), the aeolian transport of sand particles is decreased dramatically by vegetation in the wide oases within the northern area (Table 1). The TOMS AI data show that in the northern hot spot, which includes the wide oases (Gao & Washington, 2009), there are weaker vegetation constraints on the emission of dust particles. Moreover, the wide oases are located at the downstream end of the Tian Shan-derived rivers and on relatively low and flat terrain, which is also conducive to the accumulation of dust-sized particles (Langford, 1989). Therefore, there are extensive areas of fine-grained sediments in the oases, such as silt-rich fluvial deposits and soils (aggregates of clay and silt). The fluvial sediment sample, collected from the oases, has a dust fraction content of >20%, which is much larger than that of samples from other types (Figure 2). Thus, in addition to direct aerodynamic lifting of dust particles from the oases (Sweeney & Mason, 2013), saltation bombardment and the disintegration of soil aggregates are two important mechanisms for generating dust within the oases (Shao, 2001). These two mechanisms highlight the importance of saltation for large-scale dust emission (Bristow & Moller, 2018; Shao, 2001). It is a conventional view that, worldwide, except for the Bodélé Depression, the most important mechanism of dust production is that quartz sand saltating bombards large areas of fine deposits, creating active dust hot spots (Bristow & Moller, 2018; Ginoux et al., 2001; Miller et al., 2006). A new view, based on field studies, is that most dust generation occurs by direct entrainment of dust due to the threshold friction velocity for silt less than that for sand (Sweeney & Mason, 2013). Although the primary mechanism for dust generation here needs further study, it is certain that changes in the availability of the Tian Shan-derived sand and dust particles for aeolian transport to the desert occur in the oases within the northern hot spot area. Wind transports dust particles mainly in suspension and they can easily be transported for distances of ~10^2–10^3 km (Bullard & Livingstone, 2009; Pye, 1987). Therefore, the Tian Shan-derived dust particles can be supplied to the entire desert area by aeolian transport.

5.5. Implications of the Relative Importance of Silt-Producing Mechanisms for the Desert Dust

Deserts are sediment sinks for the surrounding mountains, and they can potentially provide an environment for generating dust particles which are a major source of loess deposits (Bullard & Livingstone, 2009). However, it is difficult to draw conclusions about the relative importance of the silt-generating mechanisms, including aeolian abrasion on sand dunes, fluvial abrasion, and glacial grinding (Bullard & Livingstone, 2009; Wright et al., 1998; Yang, 1991). The traditional view is that the deserts of northwestern China are the major sources for the Chinese Loess Plateau (CLP; Liu, 1985). Some of the dust within the Taklamakan Desert rises directly from the surface of the sand sea into the upper troposphere, and some is lifted by upslope wind along the south mountains (Yumimoto et al., 2009); then, the dust is entrained by the westerlies, prevailing wind at the upper troposphere in the midlatitudes, to CLP and localities farther downwind (Shao et al., 2011; Sun, 2002). However, other possible loess sources are the northern and northeastern Tibetan Plateau, including the Qaidam Basin, Qilian Mountains, and Kunlun Mountains (Maher, 2016). Although the Taklamakan Desert dust is mainly derived from the Tian Shan and Kunlun Mountains (section 5.3), the likely major sediment provenance of the deserts of northwestern China is the northern and northeastern Tibetan Plateau (Hu & Yang, 2016; Liu & Yang, 2018). In addition, some new

views about the major sources for CLP loess were put forward (Maher, 2016; Nie et al., 2015, 2018). However, the focus of the debate on CLP loess still is the relative importance of the various silt supply pathways and the various generating mechanisms of loess particles. Any potential source cannot be discounted until it has been examined (Mahowald et al., 1999), and thus a huge literature has developed which characterizes samples from the putative sources and matches them with typical CLP loess (Maher, 2016), and these efforts are ongoing. Maher (2016) considers that assembling all available published data is the essential next step for reaching a definitive conclusion regarding the source of the CLP loess, including Nd/Sr, ^{10}Be, mineralogical, and magnetic evidence. Based on the finding that the inferences of which sources are important will depend on also considering different grain sizes classes separately, we suggest that an essential additional step is the recognition of the specific roles that the putative sources can play, which would help determine the relative importance of the various loess-generating mechanisms.

From the perspective of the Taklamakan Desert itself, the proportion of the sand fraction in the desert sediment samples is >90% (Figure 2), and this fraction mainly exhibits the provenance signature of the Kunlun Mountains. Within the desert, dust particles can be generated by aeolian abrasion on sand dunes, and thus, they would also exhibit the provenance signature of the Kunlun Mountains. Some of the desert dust particles, which also have the provenance signature of the Kunlun Mountains, are likely supplied directly by the rivers and winds, and these particles are not generated by aeolian abrasion within the desert. In addition, at least some of the desert dust particles, having the provenance signature of the Tian Shan Mountains, must also be mainly supplied directly. If this were not the case, there would be an abundance of residual Tian Shan-derived sand particles in the desert, which we do not observe. If the amount of dust generated by aeolian abrasion within the desert exceeds the dust supplied directly, the dust fraction would mainly exhibit the provenance signature of the Kunlun Mountains alone. Thus, we conclude that a major part of the desert dust is directly supplied by aeolian reworking of deposits from fluvial sources rather than by aeolian abrasion and that the latter is perhaps only a minor mechanism generation of dust-sized particles for the Taklamakan Desert.

6. Conclusions

This study shows substantially different provenances of different grain size fractions of sediments from the same localities and that those differences can lead to very different sediment source apportionment inferences. Generally, in desert sedimentary systems, where the finest grain sizes are very mobile, it is of great significance to consider grain size classes separately for correct interpretation of sediment provenance and sediment-routing mechanisms. The Taklamakan Desert sediment samples are close to graywacke in composition. They have low values of CIA (45.2–56.2) and PIA (43.9–57.9), suggesting that the processes, including weathering of the source rocks, sorting, and recycling, have had only a minor cumulative effect and should not obscure the provenance signatures. The samples have Cr/V < 1.0 and Y/Ni < 0.50, implying a >99% contribution from granitic rocks. Analysis of specific weathering trends with plots of A-CN-K, (A-K)-C-N, and La-Th-Sc, together with the CIA index, indicates that, for certain weathering trends, the desert sediment samples exhibit reverse trends from the sand fraction to the dust fraction, which enables differences in the provenance of the sand and dust fractions to be determined. A south-north trend of grain size fining and sorting, together with the spatial distribution of the finest genetically significant grain size population determined by EMMA analysis, Eu/Eu* anomalies, and K/Rb ratios, indicates that the Kunlun Mountains are the main source of the sand fraction. In contrast, the sources of the dust fraction include both the Kunlun and Tian Shan Mountains.

Shuttle Radar Topography Mission data show that almost the whole of the Taklamakan Desert lies within the potential drainage area of the Kunlun-derived rivers, which enables them to supply sediment to the desert basin. EVI data reveal a relatively low degree of vegetation cover for the areas supplying Kunlun-derived sediment, which suggests that these sediments are freely available for aeolian transport during arid phases. In contrast, the elevation gradient limits the potential for supplying the Tian Shan-derived sediment to the desert by restricting the development of the Tian Shan-derived fluvial system. Vegetation also limits the availability of the Tian Shan-derived sediment, but the magnitude of its effect differs between the sand and dust fractions. The large oases dramatically reduce the aeolian transport of the Tian Shan-derived sand in the Tarim Basin, but have less effect on the emission of dust particles. For the Taklamakan Desert, the

sediment supply mechanism for the dust fraction is more complex than for the sand fraction. Dust particles can be supplied from dust activity hot spots within the basin by aeolian transport, whereas this is not the case for the sand fraction. We consider that major part of the desert dust is directly supplied by aeolian reworking of deposits from fluvial sources, rather than produced by aeolian abrasion of sand-sized particles within the dune field of the desert.

Acknowledgments
This study was supported by the National Natural Science Foundation of China (grants 41430532 and 41672182) and the State Scientific Survey Project of China (2017FY101001, National Science & Technology Infrastructure Center of China). We are very grateful to Editor-in-Chief Amy East, Thomas Dunne, Dan Muhs and an anonymous reviewer for their very constructive comments and suggestions, to Dan Muhs and Jan Bloemendal for having duly corrected the English language, and to Deguo Zhang, Hongwei Li, Fangen Hu, Peng Liang, and Rongsheng Yang for discussions. The data for this paper can be accessed from the supporting information.

References

Allen, M. B., Vincent, S. J., & Wheeler, P. J. (1999). Late Cenozoic tectonics of the Kepingtage thrust zone: Interactions of the Tien Shan and Tarim Basin, northwest China. *Tectonics*, *18*(4), 639–654. https://doi.org/10.1029/1999TC900019

Amorosi, A., Centineo, M. C., Dinelli, E., Lucchini, F., & Tateo, F. (2002). Geochemical and mineralogical variations as indicators of provenance changes in Late Quaternary deposits of SE Po Plain. *Sedimentary Geology*, *151*(3), 273–292. https://doi.org/10.1016/S0037-0738(01)00261-5

Bagnold, R. A. (1941). *The Physics of Blown Sand and Desert Dunes*. London: Methuen.

Belly, P. Y. (1964). *Sand Movement of Wind*. Washington, DC: U.S. Army Coastal Engineering Research Center.

Blott, S. J., & Pye, K. (2001). GRADISTAT: A grain size distribution and statistics package for the analysis of unconsolidated sediments. *Earth Surface Processes and Landforms*, *26*(11), 1237–1248. https://doi.org/10.1002/esp.261

Bristow, C. S., & Moller, T. H. (2018). Testing the auto-abrasion hypothesis for dust production using diatomite dune sediments from the Bodélé Depression in Chad. *Sedimentology*, *65*(4), 1322–1330. https://doi.org/10.1111/sed.12423

Bruelheide, H., Jandt, U., Gries, D., Thomas, F. M., Foetzki, A., Buerkert, A., et al. (2003). Vegetation changes in a river oasis on the southern rim of the Taklamakan Desert in China between 1956 and 2000. *Phytocoenologia*, *33*(4), 801–818. https://doi.org/10.1127/0340-269x/2003/0033-0801

Bullard, J. E., & Livingstone, I. (2009). Dust. In A. J. Parsons, & A. D. Abrahams (Eds.), *Geomorphology of Desert Environments* (pp. 629–654). Dordrecht: Springer Netherlands.

Caracciolo, L., Le Pera, E., Muto, F., & Perri, F. (2011). Sandstone petrology and mudstone geochemistry of the Peruc–Korycany Formation (Bohemian Cretaceous Basin, Czech Republic). *International Geology Review*, *53*(9), 1003–1031. https://doi.org/10.1080/00206810903429011

Chang, Q., Mishima, T., Yabuki, S., Takahashi, Y., & Shimizu, H. (2000). Sr and Nd isotope ratios and REE abundances of moraines in the mountain areas surrounding the Taklimakan Desert, NW China. *Geochemical Journal*, *34*(6), 407–427. https://doi.org/10.2343/geochemj.34.407

Chen, J., Li, G., Yang, J., Rao, W., Lu, H., Balsam, W., et al. (2007). Nd and Sr isotopic characteristics of Chinese deserts: Implications for the provenances of Asian dust. *Geochimica et Cosmochimica Acta*, *71*(15), 3904–3914. https://doi.org/10.1016/j.gca.2007.04.033

Didan, K. (2015). MOD13Q1 MODIS/Terra vegetation indices 16-day L3 global 250 m SIN grid V006 [July 28, 2018]. NASA EOSDIS LP DAAC. https://doi.org/10.5067/MODIS/MOD13Q1.006

Draut, A. E., Redsteer, M. H., & Amoroso, L. (2012). Vegetation, substrate, and eolian sediment transport at Teesto Wash, Navajo Nation, 2009–2012. U.S. Department of the Interior, U.S. Geological Survey. http://pubs.usgs.gov/sir/2012/5095/

Fedo, C. M., Wayne Nesbitt, H., & Young, G. M. (1995). Unraveling the effects of potassium metasomatism in sedimentary rocks and paleosols, with implications for paleoweathering conditions and provenance. *Geology*, *23*(10), 921. https://doi.org/10.1130/0091-7613(1995)023<0921:uteopm>2.3.co;2

Folk, R. L., & Ward, W. C. (1957). Brazos River bar: A study in the significance of grain size parameters. *Journal of Sedimentary Petrology*, *27*, 3–26.

Fryberger, S. G., & Dean, G. (1979). Dunes forms and wind regime. In E. D. McKee (Ed.), *A Study of Global Sand Seas*, *Geological Survey Professional Paper* (Vol. 1052, pp. 137–170). Washington, DC: U.S. Government Printing Office.

Gao, H., & Washington, R. (2009). The spatial and temporal characteristics of TOMS AI over the Tarim Basin, China. *Atmospheric Environment*, *43*(5), 1106–1115. https://doi.org/10.1016/j.atmosenv.2008.11.013

Garzanti, E., Andò, S., & Vezzoli, G. (2009). Grain-size dependence of sediment composition and environmental bias in provenance studies. *Earth and Planetary Science Letters*, *277*(3), 422–432. https://doi.org/10.1016/j.epsl.2008.11.007

Garzanti, E., Andò, S., Vezzoli, G., Lustrino, M., Boni, M., & Vermeesch, P. (2012). Petrology of the Namib Sand Sea: Long-distance transport and compositional variability in the wind-displaced Orange Delta. *Earth-Science Reviews*, *112*(3-4), 173–189. https://doi.org/10.1016/j.earscirev.2012.02.008

Ginoux, P., Chin, M., Tegen, I., Prospero, J. M., Holben, B., Dubovik, O., & Lin, S.-J. (2001). Sources and distributions of dust aerosols simulated with the GOCART model. *Journal of Geophysical Research*, *106*(D17), 20,255–20,273. https://doi.org/10.1029/2000JD000053

Goudie, A., & Middleton, N. J. (2006). *Desert Dust in the Global System*. New York: Springer Science & Business Media.

Goudie, A. S. (2002). *Great Warm Deserts of the World: Landscapes and Evolution*. Oxford: Oxford University Press.

Goudie, A. S. (2013). *Arid and Semi-Arid Geomorphology*. New York: Cambridge University Press.

Hattori, Y., Suzuki, K., Honda, M., & Shimizu, H. (2003). Re-Os isotope systematics of the Taklimakan Desert sands, moraines and river sediments around the taklimakan desert, and of Tibetan soils. *Geochimica et Cosmochimica Acta*, *67*(6), 1203–1213. https://doi.org/10.1016/s0016-7037(02)01206-1

Hiscott, R. N. (1984). Ophiolitic source rocks for Taconic-age flysch: Trace-element evidence. *GSA Bulletin*, *95*(11), 1261–1267. https://doi.org/10.1130/0016-7606(1984)95<1261:OSRFTF>2.0.CO;2

Honda, M., & Shimizu, H. (1998). Geochemical, mineralogical and sedimentological studies on the Taklimakan Desert sands. *Sedimentology*, *45*(6), 1125–1143.

Hu, F., & Yang, X. (2016). Geochemical and geomorphological evidence for the provenance of aeolian deposits in the Badain Jaran Desert, northwestern China. *Quaternary Science Reviews*, *131*, 179–192. https://doi.org/10.1016/j.quascirev.2015.10.039

Jackson, S. E., Pearson, N. J., Griffin, W. L., & Belousova, E. A. (2004). The application of laser ablation-inductively coupled plasma-mass spectrometry to in situ U–Pb zircon geochronology. *Chemical Geology*, *211*(1-2), 47–69. https://doi.org/10.1016/j.chemgeo.2004.06.017

Jiang, X., Jin, Y., & McNutt, M. K. (2004). Lithospheric deformation beneath the Altyn Tagh and West Kunlun faults from recent gravity surveys. *Journal of Geophysical Research*, *109*, B05406. https://doi.org/10.1029/2003JB002444

Jickells, T. D., An, Z. S., Andersen, K. K., Baker, A. R., Bergametti, G., Brooks, N., et al. (2005). Global iron connections between desert dust, ocean biogeochemistry, and climate. *Science*, *308*(5718), 67–71. https://doi.org/10.1126/science.1105959

Jonell, T. N., Li, Y., Blusztajn, J., Giosan, L., & Clift, P. D. (2018). Signal or noise? Isolating grain size effects on Nd and Sr isotope variability in Indus delta sediment provenance. *Chemical Geology*, *485*, 56–73. https://doi.org/10.1016/j.chemgeo.2018.03.036

Kao, H., Gao, R., Rau, R.-J., Shi, D., Chen, R.-Y., Guan, Y., & Wu, F. T. (2001). Seismic image of the Tarim basin and its collision with Tibet. *Geology*, *29*(7), 575–578. https://doi.org/10.1130/0091-7613(2001)029<0575:SIOTTB>2.0.CO;2

Kocurek, G., & Lancaster, N. (1999). Aeolian system sediment state: Theory and Mojave Desert Kelso dune field example. *Sedimentology*, *46*(3), 505–515. https://doi.org/10.1046/j.1365-3091.1999.00227.x

Laceby, J. P., Evrard, O., Smith, H. G., Blake, W. H., Olley, J. M., Minella, J. P. G., & Owens, P. N. (2017). The challenges and opportunities of addressing particle size effects in sediment source fingerprinting: A review. *Earth-Science Reviews*, *169*, 85–103. https://doi.org/10.1016/j.earscirev.2017.04.009

Lancaster, N. (1995). *Geomorphology of Desert Dunes*. New York: Routledge.

Lancaster, N. (2013). Sand seas and dune fields. In J. Shroder (Editor in Chief), N. Lancaster, D. J. Sherman, A. C. W. Baas (Eds.) *Treatise on Geomorphology: Aeolian Geomorphology* (Vol. 11, pp. 219-245). San Diego, CA: Academic Press.

Lancaster, N., Baas, A. C. W., & Sherman, D. J. (2013). Aeolian geomorphology: Introduction. In J. Shroder (Editor in Chief), N. Lancaster, D. J. Sherman, A. C. W. Baas (Eds.) *Treatise on Geomorphology: Aeolian Geomorphology* (Vol. 11, pp. 1-6). San Diego, CA: Academic Press.

Lancaster, N., Baker, S., Bacon, S., & McCarley-Holder, G. (2015). Owens Lake dune fields: Composition, sources of sand, and transport pathways. *Catena*, *134*, 41–49. https://doi.org/10.1016/j.catena.2015.01.003

Lancaster, N., & Ollier, C. D. (1983). Sources of sand for the Namib Sand Sea. Zeitschrift fur Geomorphologie, Supplementband(45), 71–83.

Lancaster, N., Wolfe, S., Thomas, D., Bristow, C., Bubenzer, O., Burrough, S., et al. (2016). The INQUA dunes atlas chronologic database. *Quaternary International*, *410*, 3–10. https://doi.org/10.1016/j.quaint.2015.10.044

Langford, R. P. (1989). Fluvial-aeolian interactions: Part I, Modern systems. *Sedimentology*, *36*(6), 1023–1035. https://doi.org/10.1111/j.1365-3091.1989.tb01540.x

Langford, R. P., Gill, T. E., & Jones, S. B. (2016). Transport and mixing of eolian sand from local sources resulting in variations in grain size in a gypsum dune field, white sands, New Mexico, USA. *Sedimentary Geology*, *333*, 184–197. https://doi.org/10.1016/j.sedgeo.2015.12.010

Li, J., Okin, G. S., Herrick, J. E., Belnap, J., Miller, M. E., Vest, K., & Draut, A. E. (2013). Evaluation of a new model of aeolian transport in the presence of vegetation. *Journal of Geophysical Research: Earth Surface*, *118*, 288–306. https://doi.org/10.1002/jgrf.20040

Liu, Q., & Yang, X. (2018). Geochemical composition and provenance of aeolian sands in the Ordos Deserts, northern China. *Geomorphology*, *318*, 354–374. https://doi.org/10.1016/j.geomorph.2018.06.017

Liu, T. (1985). *Loess and the Environment*. Beijing: China Ocean Press.

Liu, Z., & Yang, X. (2013). Geochemical-geomorphological evidence for the provenance of aeolian sands and sedimentary environments in the Hunshandake Sandy Land, eastern Inner Mongolia, China. *Acta Geologica Sinica (English Edition)*, *87*(3), 801–840.

Ma, L., Qiao, X., Min, L., Fan, B., & Ding, X. (2002). *Altas of Chinese Geology* [in Chinese]. Beijing: Geological Publishing House.

Maher, B. A. (2016). Palaeoclimatic records of the loess/palaeosol sequences of the Chinese Loess Plateau. *Quaternary Science Reviews*, *154*, 23–84. https://doi.org/10.1016/j.quascirev.2016.08.004

Mahowald, N., Kohfeld, K., Hansson, M., Balkanski, Y., Harrison, S. P., Prentice, I. C., et al. (1999). Dust sources and deposition during the Last Glacial Maximum and current climate: A comparison of model results with paleodata from ice cores and marine sediments. *Journal of Geophysical Research*, *104*(D13), 15,895–15,916. https://doi.org/10.1029/1999JD900084

Mason, B. H., & Moore, C. B. (1982). *Principles of Geochemistry*. New York: Wiley.

McLennan, S. M. (1989). Rare earth elements in sedimentary rocks; influence of provenance and sedimentary processes. *Reviews in Mineralogy and Geochemistry*, *21*(1), 169–200.

McLennan, S. M. (1993). Weathering and global denudation. *The Journal of Geology*, *101*(2), 295–303. https://doi.org/10.1086/648222

McLennan, S. M., Hemming, S., McDaniel, D. K., & Hanson, G. N. (1993). Geochemical approaches to sedimentation, provenance, and tectonics. In M. J. Johnsson & A. Basu (Eds.), *Processes Controlling the Composition of Clastic Sediments*, *Geological Society of America Special Papers* (pp. 21–40). https://doi.org/10.1130/spe284-p21

McTainsh, G., Livingstone, I., & Strong, C. (2013). Fundamentals of aeolian sediment transport: Aeolian sediments. In J. Shroder (Editor in Chief), N. Lancaster, D. J. Sherman, A. C. W. Baas (Eds.) *Treatise on Geomorphology: Aeolian Geomorphology* (Vol. 11, pp. 23-42). San Diego, CA: Academic Press.

Miller, R. L., Cakmur, R. V., Perlwitz, J., Geogdzhayev, I. V., Ginoux, P., Koch, D., et al. (2006). Mineral dust aerosols in the NASA Goddard Institute for Space Sciences ModelE atmospheric general circulation model. *Journal of Geophysical Research*, *111*, D06208. https://doi.org/10.1029/2005jd005796

Muhs, D. R. (2017). Evaluation of simple geochemical indicators of aeolian sand provenance: Late Quaternary dune fields of North America revisited. *Quaternary Science Reviews*, *171*, 260–296. https://doi.org/10.1016/j.quascirev.2017.07.007

Muhs, D. R. (2018). The geochemistry of loess: Asian and North American deposits compared. *Journal of Asian Earth Sciences*, *155*, 81–115. https://doi.org/10.1016/j.jseaes.2017.10.032

Muhs, D. R., Bettis, E. A., Aleinikoff, J. N., McGeehin, J. P., Beann, J., Skipp, G., et al. (2008). Origin and paleoclimatic significance of late Quaternary loess in Nebraska: Evidence from stratigraphy, chronology, sedimentology, and geochemistry. *GSA Bulletin*, *120*(11-12), 1378–1407. https://doi.org/10.1130/B26221.1

Muhs, D. R., Budahn, J. R., Johnson, D. L., Reheis, M., Beann, J., Skipp, G., et al. (2008). Geochemical evidence for airborne dust additions to soils in Channel Islands National Park, California. *GSA Bulletin*, *120*(1-2), 106–126. https://doi.org/10.1130/B26218.1

Muhs, D. R., Lancaster, N., & Skipp, G. L. (2017). A complex origin for the Kelso Dunes, Mojave National Preserve, California, USA: A case study using a simple geochemical method with global applications. *Geomorphology*, *276*, 222–243. https://doi.org/10.1016/j.geomorph.2016.10.002

Muhs, D. R., Roskin, J., Tsoar, H., Skipp, G., Budahn, J. R., Sneh, A., et al. (2013). Origin of the Sinai–Negev erg, Egypt and Israel: mineralogical and geochemical evidence for the importance of the Nile and sea level history. *Quaternary Science Reviews*, *69*, 28–48. https://doi.org/10.1016/j.quascirev.2013.02.022

Nesbitt, H. W., & Young, G. M. (1982). Early Proterozoic climates and plate motions inferred from major element chemistry of lutites. *Nature*, *299*, 715. https://doi.org/10.1038/299715a0

Nesbitt, H. W., Young, G. M., McLennan, S. M., & Keays, R. R. (1996). Effects of chemical weathering and sorting on the petrogenesis of siliciclastic sediments, with implications for provenance studies. *The Journal of Geology*, *104*(5), 525–542. https://doi.org/10.1086/629850

Nickling, W. G., & Neuman, C. K. (2009). Aeolian sediment transport. In A. J. Parsons & A. D. Abrahams (Eds.), *Geomorphology of Desert Environments* (pp. 517–555). Dordrecht, Netherlands: Springer.

Nie, J., Pullen, A., Garzione, C. N., Peng, W., & Wang, Z. (2018). Pre-Quaternary decoupling between Asian aridification and high dust accumulation rates. *Science Advances*, *4*(2), eaao6977. https://doi.org/10.1126/sciadv.aao6977

Nie, J., Stevens, T., Rittner, M., Stockli, D., Garzanti, E., Limonta, M., et al. (2015). Loess Plateau storage of Northeastern Tibetan Plateau-derived Yellow River sediment. *Nature Communications*, *6*(1), 8511. https://doi.org/10.1038/ncomms9511

Okin, G. S. (2013). Linked aeolian-vegetation systems. In J. Shroder (Editor in Chief), N. Lancaster, D. J. Sherman, A. C. W. Baas (Eds.) *Treatise on Geomorphology: Aeolian Geomorphology* (Vol. 11, pp. 428-439). San Diego, CA: Academic Press.

Paterson, G. A., & Heslop, D. (2015). New methods for unmixing sediment grain size data. *Geochemistry, Geophysics, Geosystems*, *16*, 4494–4506. https://doi.org/10.1002/2015GC006070

Perri, F., Critelli, S., Martín-Algarra, A., Martín-Martín, M., Perrone, V., Mongelli, G., & Zattin, M. (2013). Triassic redbeds in the Malaguide Complex (Betic Cordillera—Spain): Petrography, geochemistry and geodynamic implications. *Earth-Science Reviews*, *117*, 1–28. https://doi.org/10.1016/j.earscirev.2012.11.00

Pettijohn, F. J., Potter, P. E., & Siever, R. (1972). *Sand and Sandstone*. New York: Springer.

Pye, K. (1987). *Aeolian Dust and Dust Deposits*. London: Academic Press.

Qian, W., Quan, L., & Shi, S. (2002). Variations of the dust storm in China and its climatic control. *Journal of Climate*, *15*(10), 1216–1229. https://doi.org/10.1175/1520-0442(2002)015<1216:votdsi>2.0.co;2

Rao, W., Tan, H., Chen, J., Ji, J., Chen, Y., Pan, Y., & Zhang, W. (2015). Nd–Sr isotope geochemistry of fine-grained sands in the basin-type deserts, West China: Implications for the source mechanism and atmospheric transport. *Geomorphology*, *246*, 458–471. https://doi.org/10.1016/j.geomorph.2015.06.043

Rittner, M., Vermeesch, P., Carter, A., Bird, A., Stevens, T., Garzanti, E., et al. (2016). The provenance of Taklamakan desert sand. *Earth and Planetary Science Letters*, *437*, 127–137. https://doi.org/10.1016/j.epsl.2015.12.036

Sawyer, E. W. (1986). The influence of source rock type, chemical weathering and sorting on the geochemistry of clastic sediments from the Quetico Metasedimentary Belt, Superior Province, Canada. *Chemical Geology*, *55*(1), 77–95. https://doi.org/10.1016/0009-2541(86)90129-4

Shao, Y. (2001). A model for mineral dust emission. *Journal of Geophysical Research*, *106*(D17), 20,239–20,254. https://doi.org/10.1029/2001JD900171

Shao, Y., Wyrwoll, K. H., Chappell, A., Huang, J., Lin, Z., McTainsh, G. H., et al. (2011). Dust cycle: An emerging core theme in Earth system science. *Aeolian Research*, *2*(4), 181–204. https://doi.org/10.1016/j.aeolia.2011.02.001

Sun, J. (2002). Provenance of loess material and formation of loess deposits on the Chinese Loess Plateau. *Earth and Planetary Science Letters*, *203*(3), 845–859. https://doi.org/10.1016/S0012-821X(02)00921-4

Sweeney, M. R., & Mason, J. A. (2013). Mechanisms of dust emission from Pleistocene loess deposits, Nebraska, USA. *Journal of Geophysical Research: Earth Surface*, *118*, 1460–1471. https://doi.org/10.1002/jgrf.20101

Taylor, S. R., & McLennan, S. M. (1985). *The Continental Crust: Its Composition and Evolution*. Oxford: Blackwell.

Taylor, S. R., & McLennan, S. M. (2008). *Planetary Crusts: Their Composition, Origin and Evolution*. Cambridge: Cambridge University Press.

Thomas, D.S.G. (2013). Aeolian paleoenvironments of desert landscapes. In J. Shroder (Editor in Chief), N. Lancaster, D. J. Sherman, A. C. W. Baas (Eds.) *Treatise on Geomorphology: Aeolian Geomorphology* (Vol. 11, pp. 356-374). San Diego, CA: Academic Press.

USGS (2004). Shuttle radar topography mission, 3 arc second scene SRTM, unfilled unfinished 2.0. Global Land Cover Facility. University of Maryland, College Park, Maryland. Satellite image captured February 2000.

Wang, L., D'Odorio, P., Evans, J., Eldridge, D., McCabe, M., Caylor, K., & King, E. (2012). Dryland ecohydrology and climate change: Critical issues and technical advances. *Hydrology and Earth System Sciences*, *16*, 2585–2603. https://doi.org/10.5194/hess-16-2585-2012

Weltje, G. J., & Prins, M. A. (2007). Genetically meaningful decomposition of grain-size distributions. *Sedimentary Geology*, *202*(3), 409–424. https://doi.org/10.1016/j.sedgeo.2007.03.007

Williams, M. (2014). *Climate Change in Deserts*. Cambridge: Cambridge University Press.

Williams, M. (2015). Interactions between fluvial and eolian geomorphic systems and processes: Examples from the Sahara and Australia. *Catena*, *134*, 4–13. https://doi.org/10.1016/j.catena.2014.09.015

Wolfe, S. A., & Nickling, W. G. (1993). The protective role of sparse vegetation in wind erosion. *Progress in Physical Geography*, *17*(1), 50–68. https://doi.org/10.1177/030913339301700104

Wright, J., Smith, B., & Whalley, B. (1998). Mechanisms of loess-sized quartz silt production and their relative effectiveness: laboratory simulations. *Geomorphology*, *23*(1), 15–34. https://doi.org/10.1016/S0169-555X(97)00084-6

Yang, X. (1991). *Geomorphologische Untersuchungen in den Trockenräumen NW-Chinas unter besonderer Berücksichtigung von Badanjilin und Takelamagan*, *Göttinger Geographische Abhandlungen (GGA)* (Vol. 96). Göttingen: Verlag Erich Goltze.

Yang, X., & Eitel, B. (2016). Understanding the interactions between climate change, landscape evolution, surface processes and tectonics in the Earth System: What can the studies of Chinese deserts contribute? *Acta Geologica Sinica (English Edition)*, *90*(4), 1444–1454. https://doi.org/10.1111/1755-6724.12778

Yang, X., Liu, Z., Zhang, F., White, P. D., & Wang, X. (2006). Hydrological changes and land degradation in the southern and eastern Tarim basin, Xinjiang, China. *Land Degradation & Development*, *17*(4), 381–392. https://doi.org/10.1002/ldr.744

Yang, X., Preusser, F., & Radtke, U. (2006). Late Quaternary environmental changes in the Taklamakan Desert, western China, inferred from OSL-dated lacustrine and aeolian deposits. *Quaternary Science Reviews*, *25*(9), 923–932. https://doi.org/10.1016/j.quascirev.2005.06.008

Yang, X., Zhu, B., & White, P. D. (2007). Provenance of aeolian sediment in the Taklamakan Desert of western China, inferred from REE and major-elemental data. *Quaternary International*, *175*(1), 71–85. https://doi.org/10.1016/j.quaint.2007.03.005

Ye, Z., Chen, Y., & Zhang, X. (2014). Dynamics of runoff, river sediments and climate change in the upper reaches of the Tarim River, China. *Quaternary International*, *336*, 13–19. https://doi.org/10.1016/j.quaint.2013.06.006

Yu, G.-A., Disse, M., Huang, H. Q., Yu, Y., & Li, Z. (2016). River network evolution and fluvial process responses to human activity in a hyper-arid environment—Case of the Tarim River in Northwest China. *Catena*, *147*, 96–109. https://doi.org/10.1016/j.catena.2016.06.038

Yumimoto, K., Eguchi, K., Uno, I., Takemura, T., Liu, Z., Shimizu, A., & Sugimoto, N. (2009). An elevated large-scale dust veil from the Taklimakan Desert: Intercontinental transport and three-dimensional structure as captured by CALIPSO and regional and global models. *Atmospheric Chemistry and Physics*, *9*(21), 8545–8558. https://doi.org/10.5194/acp-9-8545-2009

Zhu, Z., Chen, Z., Wu, Z., Li, J., Li, B., & Wu, G. (1981). *Study on the Geomorphology of Wind-Drift Sands in the Taklamakan Desert* [in Chinese]. Beijing: Science Press.